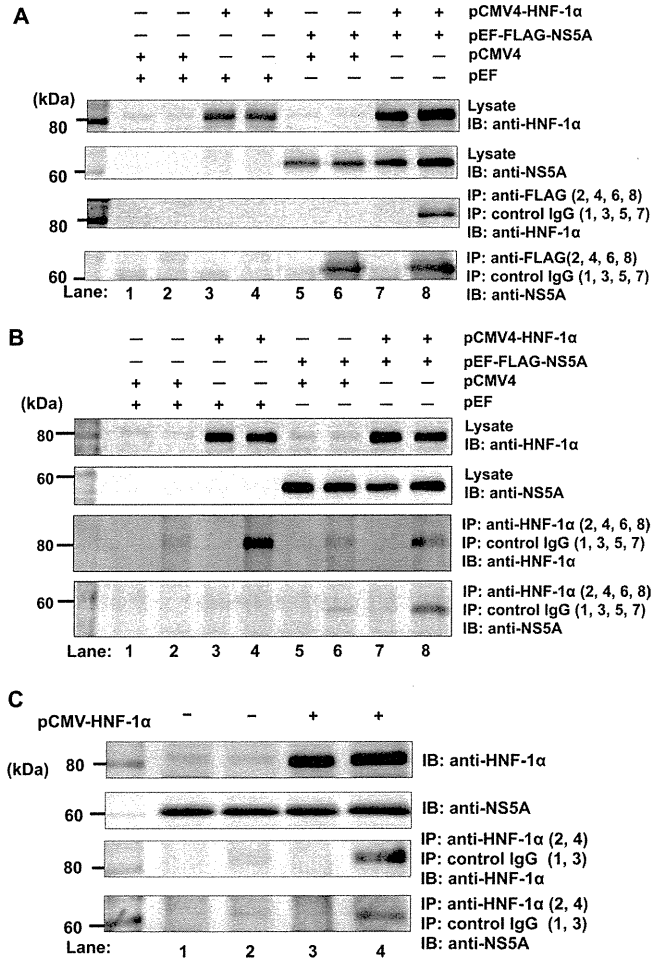


**FIG 6** NS5A protein interacts with HNF-1α protein. (A) Huh-7.5 cells were plated at $1.2 \times 10^6$ cells/10-cm dish and cultured for 12 h. Cells were transfected with plasmids as indicated. At 48 h after transfection, cells were harvested. Cell lysates were immunoprecipitated with either anti-FLAG mouse MAb (lanes 2, 4, 6, and 8) or control IgG (lanes 1, 3, 5, and 7), and bound proteins were immunoblotted with anti-HNF-1α rabbit PAb (third blot) or anti-NS5A mouse MAb (fourth blot). Protein expression of HNF-1α or FLAG-NS5A was confirmed using the same cell lysates by immunoblotting with either anti-HNF-1α rabbit PAb (first blot) or anti-NS5A mouse MAb (second blot). (B) Cell lysates were immunoprecipitated with either anti-HNF-1α rabbit PAb (lanes 2, 4, 6, and 8) or control IgG (lanes 1, 3, 5, and 7), and bound proteins were immunoblotted with either anti-HNF-1α rabbit PAb (third blot) and anti-NS5A mouse MAb (fourth blot). (C) Full-genome replicon Con1 (RCYM1) cells were plated at $1.2 \times 10^6$ cells/10-cm plate and transfected with or without pCMV-HNF-1α plasmid and cultured for 48 h. Cells were harvested and assayed for immunoprecipitation with anti-HNF-1α rabbit PAb (lanes 2 and 4) or control IgG (lanes 1 and 3). Bound proteins were immunoblotted with anti-HNF-1α goat PAb (third blot) or anti-NS5A mouse MAb (fourth blot). Input samples were immunoblotted with either anti-HNF-1α PAb (first blot) or anti-NS5A MAb (second blot). IP, immunoprecipitation; IB, immunoblotting.

1α-binding site on NS5A protein, coimmunoprecipitation analyses were performed. By use of a panel of NS5A deletion mutants (Fig. 7A), FLAG-HNF-1α protein was found to coimmunoprecipitate with all of the HA-NS5A proteins except HA-NS5A consisting of aa 357 to 447 [HA-NS5A(357–447), HA-NS5A(250–447), or HA-NS5A(214–447) (Fig. 7B, lower left panel). These results suggest that domain I of NS5A consisting of aa 1 to 213 is important for HNF-1α binding. FLAG-HNF-1α protein was also found to coimmunoprecipitate with NS5A(1–126)-myc-$His_6$ and NS5A(1–147)-myc-$His_6$. These data led to the conclusion that the HNF-1α-binding domain of NS5A protein was aa 1 to 126.

## DISCUSSION

In this study, we aimed to clarify molecular mechanisms of HCV-induced suppression of GLUT2 gene expression. The reporter assays of the human GLUT2 promoter suggest that the HNF-1α-binding site is crucial for HCV-induced suppression of GLUT2 promoter activity (Fig. 2). HCV infection significantly reduced the levels of HNF-1α mRNA (Fig. 3A). Moreover, HCV infection remarkably decreased HNF-1α protein levels (Fig. 4A). Our results suggest that HCV infection suppresses GLUT2 gene expression via NS5A-mediated lysosomal degradation of HNF-1α protein (Fig. 5). Immunoprecipitation analyses revealed that NS5A protein physically interacts with HNF-1α protein (Fig. 6) and that domain I of NS5A is important for HNF-1α binding (Fig. 7). Taken together, our results suggest that HCV infection suppresses GLUT2 transcription via downregulation of HNF-1α expression at both transcriptional and translational levels (Fig. 8).

We demonstrated that HNF-1α protein levels were greatly reduced compared to the reduced levels of HNF-1α mRNA. We demonstrated that pepstatin A, but not E64-d, restored the levels of HNF-1α protein, suggesting that an aspartic protease is involved in the degradation of HNF-1α protein. Pepstatin A is widely used for investigation of autophagy and lysosomal degradation. Further studies are needed to elucidate how HCV induces lysosomal degradation of HNF-1α protein and how HNF-1α protein is selectively downregulated by HCV infection. Our data suggest that the HCV NS5A protein is responsible for the HCV-induced degradation of HNF-1α protein. Using a panel of NS5A deletion mutants, we demonstrated that domain I of NS5A is important for association with HNF-1α protein. NS5A domain I is relatively conserved among HCV genotypes compared to domains II and III, suggesting that NS5A–HNF-1α interaction is common to all the HCV genotypes. Domain I coordinates a single zinc atom per protein molecule and is essential for HCV RNA replication (35). The crystal structure of NS5A domain I revealed the presence of a zinc coordination motif and a C-terminal disulfide bond (36). NS5A domain I was found to bind many host proteins, RNA, and membranes (16). It is possible that physical interaction between NS5A protein and HNF-1α protein is important for selective degradation of HNF-1α protein. One possible mechanism is that NS5A protein may recruit HNF-1α protein to the lysosome. Further study is necessary to test this possibility.

We observed that deletion of the GLUT2 transcriptional start site enhances expression of the GLUT2 reporter in FGR cells (Fig. 2B). Cha et al. (7) previously reported that deletion down to nucleotide +73 of the GLUT2 promoter resulted in a marked increase and that further deletion to nucleotide +188 caused a drastic decrease in luciferase activity, indicating the presence of negative- and positive-regulator elements in the 5′ untranslated region. The role of these elements in HCV-infected cells remains to be elucidated.

We demonstrated that HCV J6/JFH1 infection reduced the HNF-1α mRNA level and HNF-1α protein level. Our results contradict an earlier report (32) demonstrating that expression of HNF-1 mRNA was increased in subgenomic replicon Huh.8 cells (3). We observed downregulation of HNF-1α mRNA and

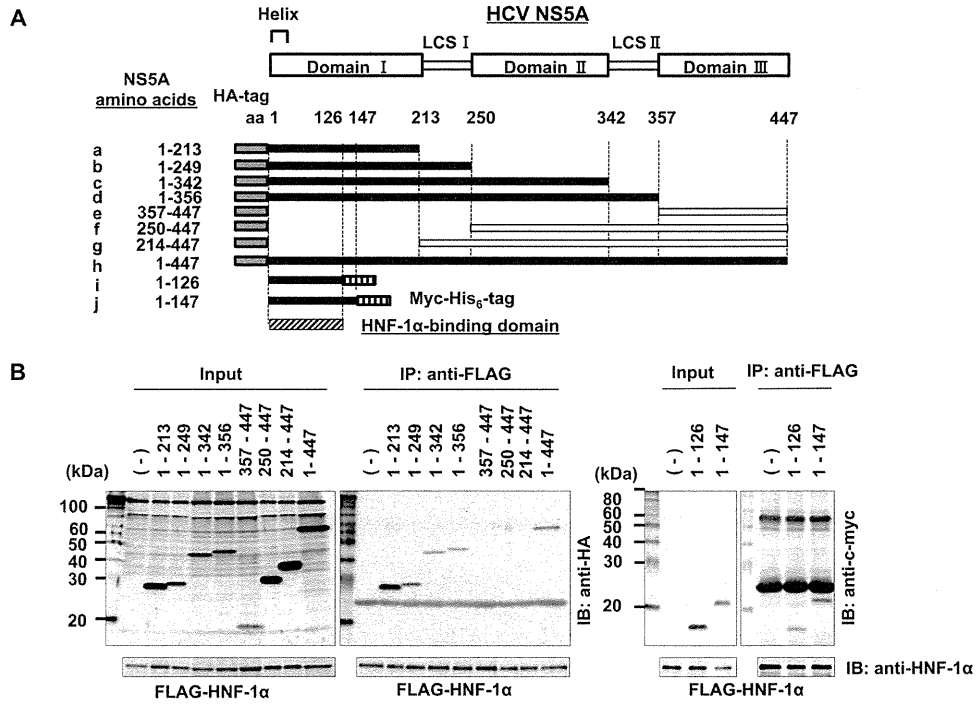


FIG 7 Mapping of the HNF-1α-binding domain for NS5A protein. (A) Schematic representation of the hepatitis C virus NS5A protein. NS5A consists of three domains (domains I, II, and III) with domains separated by low-complexity sequences (LCS I and II). The position of the amino-terminal amphipathic helix membrane anchor is shown (labeled helix). The NS5A deletion mutants (a to j) contain the NS5A amino acids indicated to the left. Each NS5A deletion mutant contains either HA tag in the N terminus (a to h) or myc-$His_6$ tag in the C terminus (i and j). The gray region of each represents the HA tag sequence. The lattice region of each represents the myc-$His_6$ tag (i and j). Closed boxes represent proteins that are bound specifically to HNF-1α protein, and open boxes represent those that are not bound. (B) Huh-7.5 cells were transfected with each NS5A mutant plasmid together with a FLAG-HNF-1α expression plasmid. At 48 h posttransfection, cells were harvested, and cell lysates were immunoprecipitated with anti-FLAG beads. Input samples and immunoprecipitated samples were immunoblotted with anti-HA MAb (two left panels, top), anti-c-myc MAb (two right panels, top), or anti-HNF-1α PAb (all panels, bottom).

HNF-1α protein in SGR cells as well as in FGR cells (data not shown). We also demonstrated that the ectopic expression of NS5A protein decreased the endogenous HNF-1α protein level. The reasons for these discrepancies remain to be elucidated.

We along with other groups previously reported that HCV NS5A protein is involved in mitochondrial reactive oxygen species (ROS) production (11, 13, 38). Mitochondrial ROS generation is known to induce the autophagy pathway (22) and lysosomal membrane permeabilization (8). Therefore, it is necessary to determine whether NS5A-induced ROS production enhances autophagic degradation or lysosomal membrane permeabilization. Several groups have reported that autophagy vesicles accumulate in HCV-infected cells and that autophagy proteins can function as proviral factors required for HCV replication (14). Autophagy degrades macromolecules and organelles. Based on the means by which cargo is delivered to the lysosomes, three different autophagy pathways are described: macroautophagy, microautophagy, and chaperone-mediated autophagy (CMA). At first, autophagy was considered a nonselective bulk degradation process. CMA, however, results in specific degradation of the cytosolic proteins in a molecule-by-molecule fashion. Most known substrates for CMA contain a peptide sequence biochemically related to KFERQ (12). Although the typical KFERQ peptide motif is not found in HNF-1α protein, it is possible that KFERQ-like sequences can be generated by post-translational modifications. It is also possible that HNF-1α protein possesses other degradation motifs. The molecular mechanism underlying NS5A-dependent lysosomal degradation of HNF-1α protein needs to be elucidated.

HNF-1α is a homeodomain-containing transcription factor, which is expressed in the liver, pancreatic β cells, and other tissues (1). Intriguingly, HNF-1α is known to play a crucial role in diabetes. Heterozygous germ line mutations in the gene encoding HNF-1α are responsible for an autosomal dominant form of non-insulin-dependent diabetes, MODY3 (40). Mutations in the HNF-1α gene disrupt GLUT2 function as a glucose sensor in pancreatic β cells, resulting in severe insulin secretory defects (39). It is unclear whether HNF-1α mutations in the liver affect glucose homeostasis in MODY3 patients. Two strains of HNF-1α-deficient mice have been reported. The mice of the first strain, created using standard methods for making knockout mice, are born normally, but most die postnatally around the weaning period after a progressive wasting syndrome (31). Mice of the second strain, created using the Cre-loxP recombination method, had a normal life span (20). The knockout mice of the second strain were dwarfed, diabetic, and infertile. Moreover, the knockout mice had enlarged livers and exhibited progressive liver damage.

HNF-1α was also identified as a tumor suppressor gene involved in human liver tumorigenesis since biallelic inactivating mutations of the HNF-1α gene were found in 50% of hepatocellular adenomas and, in rare cases, of well-differentiated hepatocellular carcinomas developed in the absence of cirrhosis (5).

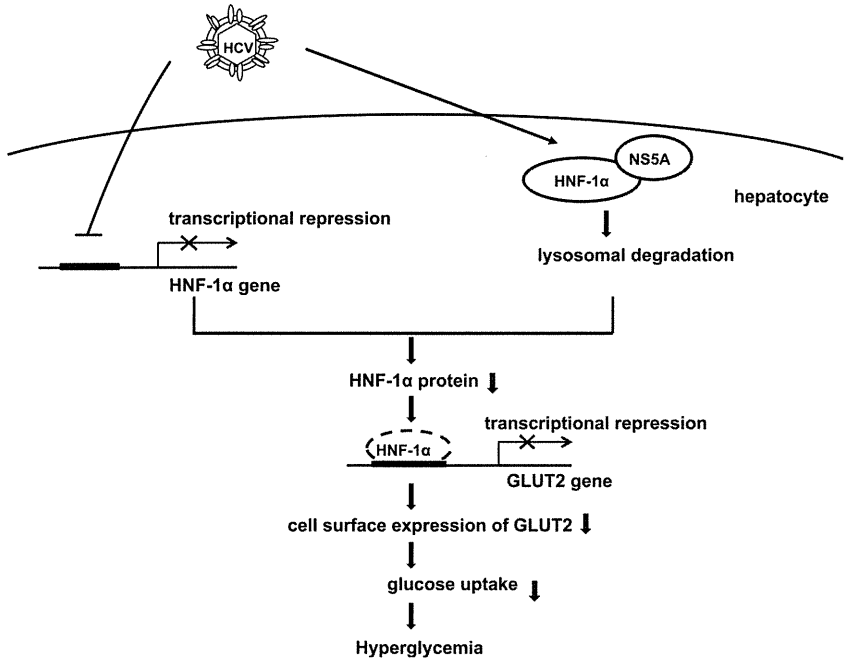


FIG 8 A proposed mechanism of the HCV-induced suppression of GLUT2 via downregulation of HNF-1α. HCV infection downregulates HNF-1α at transcriptional and posttranslational levels, resulting in suppression of GLUT2 gene transcription. HCV NS5A protein physically interacts with HNF-1α protein and enhances lysosomal degradation of HNF-1α protein.

Moreover, HNF-1α has been shown to regulate a large number of genes related to glucose, fatty acid, bile acid, cholesterol, and lipoprotein metabolisms as well as inflammation (1). Therefore, it is possible that HCV-induced downregulation of HNF-1α may play a crucial role in metabolic disorders as well as tumorigenesis.

To determine which HCV protein is involved in the suppression of the GLUT2 promoter, we examined the effects of transient expression of HCV proteins on GLUT2 promoter activity. Overexpression of NS5A suppressed GLUT2 promoter activity, whereas overexpression of p7 enhanced GLUT2 promoter activity (Fig. 5A). SGR cells express NS5A protein but lack p7 protein. FGR cells express both NS5A protein and p7 protein. However, GLUT2 promoter activity was suppressed in both SGR and FGR cells (Fig. 2B). This discrepancy between transient expression system and replicon cells may result from the differences in trafficking of p7 because it is a complex process potentially regulated by both the cleavage from its upstream signal peptides and targeting signals within the protein sequence (15).

We previously reported that HCV infection promotes hepatic gluconeogenesis in HCV J6/JFH1-infected Huh-7.5 cells (11). HCV infection transcriptionally upregulates the genes for phosphoenolpyruvate carboxykinase (PEPCK) and glucose 6-phosphatase (G6Pase), the rate-limiting enzymes for hepatic gluconeogenesis. We demonstrated that gene expression of PEPCK and G6Pase was regulated by the transcription factor forkhead box O1 (FoxO1) in HCV-infected cells. Phosphorylation of the FoxO1 at Ser319 was markedly diminished in HCV-infected cells, resulting in increased nuclear accumulation of FoxO1. HCV NS5A protein was directly linked with FoxO1-dependent increased gluconeogenesis. HCV-induced downregulation of GLUT2 expression and upregulation of gluconeogenesis may cooperatively contribute to development of type 2 diabetes in HCV-infected patients at least to some extent. HCV-induced downregulation of GLUT2 expression and upregulation of gluconeogenesis may result in high concentrations of glucose in HCV-infected hepatocytes. As suggested in a recent study, low glucose concentrations in the hepatocytes inhibit HCV replication (28). Therefore, high glucose levels in the hepatocytes may confer an advantage in efficient replication of HCV.

In conclusion, we provided evidence suggesting that HCV infection downregulates HNF-1α expression at both transcriptional and posttranslational levels. HCV-induced downregulation of HNF-1α may play a crucial role in glucose metabolic disorders caused by HCV infection. Strategies aimed at HCV-induced downregulation of HNF-1α protein may lead to the development of new therapeutic agents for HCV-induced diabetes.

## ACKNOWLEDGMENTS

We are grateful to C. M. Rice (Rockefeller University, New York, NY) for providing Huh-7.5 cells and pFL-J6/JFH1, R. Bartenschlager (University of Heidelberg, Heidelberg, Germany) for providing an HCV subgenomic RNA replicon (pFK5B/2884Gly), and N. Kato (Okayama University, Okayama, Japan) for providing an HCV full-genome RNA replicon (pON/C-5B). We thank T. Adachi, M. Makimoto, K. Tsubaki, Y. Yasui, A. Asahi, M. Kohmoto, and Y.-H. Ide for their technical assistance. We also thank K. Hachida for secretarial work.

This work was supported in part by grants-in-aid for research on hepatitis from the Ministry of Health, Labor, and Welfare, Japan, and the Ministry of Education, Culture, Sports, Science, and Technology (MEXT), Japan. This work was also supported in part by the Japan Initiative for Global Research Network on Infectious Diseases program of MEXT, Japan. This study was also carried out as part of the Global Center of Excellence program of the Kobe University Graduate School of Medicine and the Science and Technology Research Partnership for Sustain-

able Development program of the Japan Science and Technology Agency and the Japan International Cooperation Agency.

We have no potential conflicts of interest to report.

## REFERENCES

1. **Armendariz AD, Krauss RM.** 2009. Hepatic nuclear factor 1-alpha: inflammation, genetics, and atherosclerosis. Curr. Opin. Lipidol. **20**:106–111.
2. **Ban N, et al.** 2002. Hepatocyte nuclear factor-1α recruits the transcriptional co-activator p300 on the GLUT2 gene promoter. Diabetes **51**:1409–1418.
3. **Blight KJ, Kolykhalov AA, Rice CM.** 2000. Efficient initiation of HCV RNA replication in cell culture. Science **290**:1972–1974.
4. **Blight KJ, McKeating JA, Rice CM.** 2002. Highly permissive cell lines for subgenomic and genomic hepatitis C virus RNA replication. J. Virol. **76**: 13001–13014.
5. **Bluteau O, et al.** 2002. Bi-allelic inactivation of TCF1 in hepatic adenomas. Nat. Genet. **32**:312–315.
6. **Bungyoku Y, et al.** 2009. Efficient production of infectious hepatitis C virus with adaptive mutations in cultured hepatoma cells. J. Gen. Virol. **90**:1681–1691.
7. **Cha JY, Kim H, Kim KS, Hur MW, Ahn Y.** 2000. Identification of transacting factors responsible for the tissue-specific expression of human glucose transporter type 2 isoform gene. Cooperative role of hepatocyte nuclear factors 1α and 3β. J. Biol. Chem. **275**:18358–18365.
8. **Denamur S, et al.** 2011. Role of oxidative stress in lysosomal membrane permeabilization and apoptosis induced by gentamicin, an aminoglycoside antibiotic. Free Radic. Biol. Med. **51**:1656–1665.
9. **Deng L, et al.** 2008. Hepatitis C virus infection induces apoptosis through a Bax-triggered, mitochondrion-mediated, caspase 3-dependent pathway. J. Virol. **82**:10375–10385.
10. **Deng L, et al.** 2006. NS3 protein of Hepatitis C virus associates with the tumour suppressor p53 and inhibits its function in an NS3 sequence-dependent manner. J. Gen. Virol. **87**:1703–1713.
11. **Deng L, et al.** 2011. Hepatitis C virus infection promotes hepatic gluconeogenesis through an NS5A-mediated, FoxO1-dependent pathway. J. Virol. **85**:8556–8568.
12. **Dice JF.** 2007. Chaperone-mediated autophagy. Autophagy **3**:295–299.
13. **Dionisio N, et al.** 2009. Hepatitis C virus NS5A and core proteins induce oxidative stress-mediated calcium signalling alterations in hepatocytes. J. Hepatol. **50**:872–882.
14. **Dreux M, Chisari FV.** 2011. Impact of the autophagy machinery on hepatitis C virus infection. Viruses **3**:1342–1357.
15. **Griffin S, Clarke D, McCormick C, Rowlands D, Harris M.** 2005. Signal peptide cleavage and internal targeting signals direct the hepatitis C virus p7 protein to distinct intracellular membranes. J. Virol. **79**:15525–15536.
16. **He Y, Staschke KA, Tan SL.** 2006. HCV NS5A: a multifunctional regulator of cellular pathways and virus replication. *In* Tan SL (ed), Hepatitis C viruses: genomes and molecular biology. Horizon Bioscience, Norfolk, United Kingdom. http://www.ncbi.nlm.nih.gov/books/NBK1621/.
17. **Ikeda M, et al.** 2005. Efficient replication of a full-length hepatitis C virus genome, strain O, in cell culture, and development of a luciferase reporter system. Biochem. Biophys. Res. Commun. **329**:1350–1359.
18. **Inubushi S, et al.** 2008. Hepatitis C virus NS5A protein interacts with and negatively regulates the non-receptor protein tyrosine kinase Syk. J. Gen. Virol. **89**:1231–1242.
19. **Kasai D, et al.** 2009. HCV replication suppresses cellular glucose uptake through down-regulation of cell surface expression of glucose transporters. J. Hepatol. **50**:883–894.
20. **Lee YH, Sauer B, Gonzalez FJ.** 1998. Laron dwarfism and non-insulin-dependent diabetes mellitus in the Hnf-1α knockout mouse. Mol. Cell Biol. **18**:3059–3068.
21. **Lemon SM, Walker C, Alter MJ, Yi M.** 2007. Hepatitis C virus, p 1291–1304. *In* Knipe DM, et al (ed), Fields virology, 5th ed. Lippincott Williams & Wilkins, Philadelphia, PA.
22. **Li ZY, Yang Y, Ming M, Liu B.** 2011. Mitochondrial ROS generation for regulation of autophagic pathways in cancer. Biochem. Biophys. Res. Commun. **414**:5–8.
23. **Lindenbach BD, et al.** 2005. Complete replication of hepatitis C virus in cell culture. Science **309**:623–626.
24. **Macheda ML, Rogers S, Best JD.** 2005. Molecular and cellular regulation of glucose transporter (GLUT) proteins in cancer. J. Cell Physiol. **202**: 654–662.
25. **Malecki MT, Mlynarski W.** 2008. Monogenic diabetes: implications for therapy of rare types of disease. Diabetes Obes. Metab. **10**:607–616.
26. **Mason AL, et al.** 1999. Association of diabetes mellitus and chronic hepatitis C virus infection. Hepatology **29**:328–333.
27. **Murakami K, et al.** 2006. Production of infectious hepatitis C virus particles in three-dimensional cultures of the cell line carrying the genome-length dicistronic viral RNA of genotype 1b. Virology **351**:381–392.
28. **Nakashima K, Takeuchi K, Chihara K, Hotta H, Sada K.** 2011. Inhibition of hepatitis C virus replication through adenosine monophosphate-activated protein kinase-dependent and -independent pathways. Microbiol. Immunol. **55**:774–782.
29. **Negro F.** 2011. Mechanisms of hepatitis C virus-related insulin resistance. Clin. Res. Hepatol Gastroenterol. **35**:358–363.
30. **Negro F, Alaei M.** 2009. Hepatitis C virus and type 2 diabetes. World J. Gastroenterol. **15**:1537–1547.
31. **Pontoglio M, et al.** 1996. Hepatocyte nuclear factor 1 inactivation results in hepatic dysfunction, phenylketonuria, and renal Fanconi syndrome. Cell **84**:575–585.
32. **Qadri I, et al.** 2004. Induced oxidative stress and activated expression of manganese superoxide dismutase during hepatitis C virus replication: role of JNK, p38 MAPK and AP-1. Biochem. J. **378**:919–928.
33. **Shirakura M, et al.** 2007. E6AP ubiquitin ligase mediates ubiquitylation and degradation of hepatitis C virus core protein. J. Virol. **81**:1174–1185.
34. **Takeda J, Kayano T, Fukomoto H, Bell GI.** 1993. Organization of the human GLUT2 (pancreatic beta-cell and hepatocyte) glucose transporter gene. Diabetes **42**:773–777.
35. **Tellinghuisen TL, Marcotrigiano J, Gorbalenya AE, Rice CM.** 2004. The NS5A protein of hepatitis C virus is a zinc metalloprotein. J. Biol. Chem. **279**:48576–48587.
36. **Tellinghuisen TL, Marcotrigiano J, Rice CM.** 2005. Structure of the zinc-binding domain of an essential component of the hepatitis C virus replicase. Nature **435**:374–379.
37. **Wakita T, et al.** 2005. Production of infectious hepatitis C virus in tissue culture from a cloned viral genome. Nat. Med. **11**:791–796.
38. **Wang AG, et al.** 2009. Non-structural 5A protein of hepatitis C virus induces a range of liver pathology in transgenic mice. J. Pathol. **219**:253–262.
39. **Wang H, Maechler P, Hagenfeldt KA, Wollheim CB.** 1998. Dominant-negative suppression of HNF-1alpha function results in defective insulin gene transcription and impaired metabolism-secretion coupling in a pancreatic beta-cell line. EMBO J. **17**:6701–6713.
40. **Yamagata K, et al.** 1996. Mutations in the hepatocyte nuclear factor-1α gene in maturity-onset diabetes of the young (MODY3). Nature **384**:455–458.

JCM
Journals.ASM.org

# NS5A Sequence Heterogeneity of Hepatitis C Virus Genotype 4a Predicts Clinical Outcome of Pegylated-Interferon–Ribavirin Therapy in Egyptian Patients

**Ahmed El-Shamy,[a,b]* Ikuo Shoji,[a] Wafaa El-Akel,[c] Shymaa E. Bilasy,[d] Lin Deng,[a] Maissa El-Raziky,[c] Da-peng Jiang,[a] Gamal Esmat,[c] and Hak Hotta[a]**

Division of Microbiology, Center for Infectious Diseases, Kobe University Graduate School of Medicine, Kobe, Japan[a]; Department of Virology, Suez Canal University Faculty of Veterinary Medicine, Ismalia, Egypt[b]; Department of Tropical Medicine, Cairo University, Cairo, Egypt[c]; and Department of Biochemistry, Suez Canal University Faculty of Pharmacy, Ismalia, Egypt[d]

**Hepatitis C virus genotype 4 (HCV-4) is the cause of approximately 20% of the 180 million cases of chronic hepatitis C in the world. HCV-4 infection is common in the Middle East and Africa, with an extraordinarily high prevalence in Egypt. Viral genetic polymorphisms, especially within core and NS5A regions, have been implicated in influencing the response to pegylated-interferon and ribavirin (PEG-IFN/RBV) combination therapy in HCV-1 infection. However, this has not been confirmed in HCV-4 infection. Here, we investigated the impact of heterogeneity of NS5A and core proteins of HCV-4, mostly subtype HCV-4a, on the clinical outcomes of 43 Egyptian patients treated with PEG-IFN/RBV. Sliding window analysis over the carboxy terminus of NS5A protein identified the IFN/RBV resistance-determining region (IRRDR) as the most prominent region associated with sustained virological response (SVR). Indeed, 21 (84%) of 25 patients with SVR, but only 5 (28%) of 18 patients with non-SVR, were infected with HCV having IRRDR with 4 or more mutations (IRRDR ≥ 4) ($P = 0.0004$). Multivariate analysis identified IRRDR ≥ 4 as an independent SVR predictor. The positive predictive value of IRRDR ≥ 4 for SVR was 81% (21/26; $P = 0.002$), while its negative predictive value for non-SVR was 76% (13/17; $P = 0.02$). On the other hand, there was no significant correlation between core protein polymorphisms, either at residue 70 or at residue 91, and treatment outcome. In conclusion, the present results demonstrate for the first time that IRRDR ≥ 4, a viral genetic heterogeneity, would be a useful predictive marker for SVR in HCV-4 infection when treated with PEG-IFN/RBV.**

Hepatitis C virus (HCV) is a major cause of chronic liver disease, hepatocellular carcinoma, and deaths from liver disease and is the most common indication for liver transplantation (7, 26–28, 38). HCV has been classified into seven major genotypes and a series of subtypes (35, 36). In general, HCV genotype 4 (HCV-4) is common in the Middle East and Africa, where it is responsible for more than 80% of HCV infections (23). Although HCV-4 is the cause of approximately 20% of the 180 million cases of chronic hepatitis C in the world, it has not been a major subject of research.

Egypt has the highest prevalence of HCV worldwide (15%) and the highest prevalence of HCV-4, which is responsible for 90% of the total HCV infections, with a predominance of the subtype 4a (HCV-4a) (1, 32). This extraordinarily high prevalence results in an increasing incidence of hepatocellular carcinoma in Egypt, which is now the second most frequent cause of cancer and cancer mortality among men (17, 21). More than 2 decades have passed since the discovery of HCV, and yet therapeutic options remain limited. Up to 2011, the standard treatment for chronic hepatitis C consisted of pegylated alpha interferon (PEG-IFN) and ribavirin (RBV) (19); however, by May 2011 two protease inhibitors (telaprevir and boceprevir) were approved by the Food and Drug Administration (FDA) for use in combination with PEG-IFN/RBV for adult chronic hepatitis C patients with HCV genotype 1 (24, 34). Since the approval of these new protease inhibitors for treatment of HCV-1 infection, the response of HCV-4 to the standard regimen of treatment (PEG-IFN/RBV) has lagged behind other genotypes and HCV-4 has become the most resistant genotype to treat. As PEG-IFN/RBV still remains to be used to treat HCV-4-infected patients, exploring the factors that predict the outcome of PEG-IFN/RBV treatment, such as sustained virological response (SVR), for HCV-4 infections is needed to assess more accurately the likelihood of SVR and thus to make more informed treatment decisions.

While the SVR rate for PEG-IFN/RBV treatment hovers at 50 to 60% in HCV-1 and -4 infection, it is up to 80% in HCV-2 and -3 infections (19, 33). This difference in responses among patients infected with different HCV genotypes suggests that viral genetic heterogeneity could affect, at least to some extent, the sensitivity to IFN-based therapy. In this context, the correlation between IFN-based therapy outcome and sequence polymorphisms within the viral core and NS5A proteins has been widely discussed, in particular in regard to Japanese patients with HCV-1b infection. Initially, in the era of IFN monotherapy, it was proposed that sequence variations within a region in NS5A of HCV-1b, called the IFN sensitivity-determining region (ISDR), were correlated with IFN responsiveness (18). Subsequently, in the era of PEG-IFN/

**Received** 8 August 2012 **Returned for modification** 30 August 2012
**Accepted** 14 September 2012
**Published ahead of print** 19 September 2012
Address correspondence to Hak Hotta, hotta@kobe-u.ac.jp.
* Present address: Ahmed El-Shamy, Division of Liver Diseases, Mount Sinai School of Medicine, New York, New York, USA.

doi:10.1128/JCM.02109-12

RBV combination therapy, we identified a new region near the C terminus of NS5A, referred to as the IFN/RBV resistance-determining region (IRRDR) (13). Recently, we also demonstrated the correlation between IRRDR polymorphism and PEG-IFN/RBV treatment outcome in HCV-2a and -2b infections (15). In addition, HCV core protein polymorphism, in particular at positions 70 and 91, was also proposed as a pretreatment predictor of poor virological response in patients infected with HCV-1b (4–6). To the best of our knowledge, there is no information regarding the correlation between sequence heterogeneity in the NS5A and core proteins of HCV-4 and PEG-IFN/RBV treatment outcome. In the present study, we aimed to investigate this issue in Egyptian patients infected with HCV-4.

## MATERIALS AND METHODS

**Ethics statement.** The study protocol, which conforms to the provisions of the Declaration of Helsinki, was approved beforehand by the Ethic Committees in Cairo University Hospital and in Kobe University, and written informed consent was obtained from each patient prior to the treatment.

**Patients.** A total of 43 previously untreated patients who were chronically infected with HCV-4a (34 patients), HCV-4m (3 patients), HCV-4n (3 patients), or HCV-4o (3 patients) were consecutively evaluated for antiviral treatment at Cairo University Hospital, Cairo, Egypt, between January 2008 and September 2010. The HCV subtype was determined according to the method of Okamoto et al. (31). The patients were treated with PEG-IFN α-2a (180 μg/week, subcutaneously) and RBV (1,000 to 1,200 mg daily, *per os*) for 48 weeks. The quantification of serum HCV RNA titers was performed as previously reported (14). To minimize the therapeutic burdens, including the high cost and possible side effects, therapy was discontinued if HCV RNA titers at week 12 did not drop by 2 log compared with baseline values or if HCV RNA was still detectable at week 24. These were considered a null response (see Results).

**Sequence analysis of the NS5A and core regions of the HCV genome.** Blood samples were collected using Vacutainer tubes. The sera were separated within 2 h of blood collection, transferred to sterile cryovials, and kept frozen at −80°C until use. HCV RNA was extracted from 140 μl of serum using a commercially available kit (QIAmp viral RNA kit; Qiagen, Tokyo, Japan). The extracted RNA was reverse transcribed and amplified for the HCV genome encoding a carboxy terminus of NS5A (amino acids [aa] 2193 to 2417) and the core protein (aa 1 to 191) using SuperScript III one-step RT-PCR Platinum *Taq* HiFi (Invitrogen, Tokyo, Japan). The resultant reverse transcription (RT)-PCR product was subjected to a second-round PCR by using Platinum *Taq* DNA polymerase high fidelity III (Invitrogen). Primers used for amplification of the 3′ half of the NS5A region of HCV-4 were as follows: NS5A-4/F1 (5′-CTCAAYTCGTTCGTRGTGGGATC-3′; sense) and NS5A-4/R1 (5′-CGAAGGTCACCTTCTTCTGCCG-3′; antisense) for one-step RT-PCR; and NS5A-4/F2 (5′-ATGCGAGCCYGAGCCGGACGT-3′; sense) and NS5A-4/R2 (5′-GCTCAGGGGGYTRATTGGCAGCT-3′; antisense) for the second-round PCR. Primers for amplification of the core region of HCV-4 were 249-F (5′-GCTAGCCGAGTAGTGTTG-3′; sense) and 984-R (5′-GATGTGRTGRTCGGCCTC-3′; antisense) (40) for one-step RT-PCR; and 319-F (5′-GGAGGTCTCGTAGACCGTGC-3′; sense) (40) and primer-186 (5′-ATGTACCCCATGAGGTCGGC-3′; antisense) (2) for the second-round PCR. RT was performed at 45°C for 30 min and terminated at 94°C for 2 min, followed by the first-round PCR over 35 cycles, with each cycle consisting of denaturation at 94°C for 30 s, annealing at 50°C for 30 s, and extension at 68°C for 90 s. The second-round PCR was performed under the same conditions. The sequences of the amplified fragments were determined by direct sequencing without subcloning. The amino acid sequences were deduced and aligned using Genetyx Win software version 7.0 (Genetyx Corp., Tokyo, Japan). The numbering of amino acid residues for HCV-4 isolates is according to the polyprotein of ED43 isolate (accession no. Y11604) (10). Consensus sequences of the carboxy terminus of NS5A of a given HCV-4 subtype were inferred by alignment of all sequences obtained in this study as well as all available NS5A sequences of HCV-4a (accession no. Y11604, DQ418782 to DQ418789, DQ516084, and DQ988073 to DQ988079), HCV-4m (FJ462433), HCV-4n (FJ462441), and HCV-4o (FJ462440) from the databases.

TABLE 1 Virological responses of HCV-4-infected patients treated with PEG-IFN/RBV

| Virological response | Proportion (%) of patients with indicated response (no. of patients/total no.) | | | | |
|---|---|---|---|---|---|
| | HCV-4[a] | HCV-4a | HCV-4 m | HCV-4n | HCV-4o |
| SVR | 58 (25/43) | 56 (19/34) | 100 (3/3) | 33 (1/3) | 67 (2/3) |
| Non-SVR | 42 (18/43) | 44 (15/34) | 0 (0/3) | 67 (2/3) | 33 (1/3) |
| Null response | 30 (13/43) | 32 (11/34) | 0 (0/3) | 67 (2/3) | 0 (0/3) |
| Relapse | 12 (5/43) | 12 (4/34) | 0 (0/3) | 0 (0/3) | 33 (1/3) |

[a] Includes all 43 cases with HCV-4 infection (34 cases with HCV-4a and 3 cases each with HCV-4m, -4n, and -4o).

**Statistical analysis.** Numerical data were analyzed by Student's *t* test and categorical data by Fisher's exact probability test. To evaluate the optimal threshold of the number of amino acid mutations in IRRDR for prediction of treatment outcomes, the receiver operating characteristic (ROC) curve was constructed. Univariate and multivariate logistic regression analyses were performed to identify independent predictors for treatment outcomes. All statistical analyses were performed using the SPSS version 16 software (SPSS Inc., Chicago, IL). Unless otherwise stated, a $P$ value of $<0.05$ was considered statistically significant.

**Nucleotide sequence accession numbers.** The sequence data reported in this paper have been deposited in the DDBJ/EMBL/GenBank nucleotide sequence databases with the accession numbers AB725987 through AB726066.

## RESULTS

**Patients' responses to PEG-IFN/RBV combination therapy.** Among 43 patients enrolled in this study, 30 (70%) patients completed the entire course of PEG-IFN/RBV treatment for 48 weeks and follow-up for 24 weeks. On the other hand, the treatment was discontinued for 13 (30%) patients due to poor virological responses at 12 or 24 weeks after initiation of the therapy. Overall, 25 (58%) patients achieved SVR while 18 (42%) patients had non-SVR (Table 1). When analyzed on the basis of the subtype classification, SVR was achieved by 56% (19/34), 100% (3/3), 33% (1/3), and 67% (2/3) of patients infected with HCV-4a, -4m, -4n, and -4o, respectively.

Non-SVR patients are classified into two groups: (i) patients with null response, who did not achieve >2-log reduction of the initial viral load at week 12 or who had detectable viremia at week 24 of the treatment period; and (ii) patients with relapse, who were negative for HCV-RNA at the end of the treatment period (week 48) followed by a rebound viremia at a certain time point during the follow-up period of 24 weeks. Patients with null response represented 30% (13/43) of all the HCV-4-infected subjects analyzed, while those with relapse represented 12% (5/43). A similar tendency was observed for subtype HCV-4a.

Among various patients' demographic characteristics, SVR patients had a significantly lower average age than that of non-SVR patients (Table 2). Furthermore, a tendency for SVR patients to have a lower average titer of initial viral load than that of non-SVR was noted, although the difference was not statistically significant, due possibly to the small number of patients analyzed ($P = 0.07$).

TABLE 2 Demographic characteristics of HCV-4-infected patients with SVR and non-SVR[a]

| Factor | SVR | Non-SVR | *P* value |
|---|---|---|---|
| Age | 38.47 ± 9.51 | 45.80 ± 5.65 | 0.014 |
| Sex (male/female) | 18/7 | 15/3 | 0.48 |
| BMI | 27.36 ± 3.65 | 27.67 ± 5.28 | 0.85 |
| Platelets ($\times 10^3/\mu l$) | 204.4 ± 40.63 | 216.7 ± 87.25 | 0.59 |
| Hemoglobin (g/dl) | 14.54 ± 1.38 | 15.08 ± 1.39 | 0.25 |
| WBC count | 7,041 ± 1,876 | 7,078 ± 2,977 | 0.96 |
| Albumin (g/dl) | 4.12 ± 0.36 | 4.328 ± 0.41 | 0.11 |
| ALT (IU/liter) | 78.72 ± 59.68 | 82.39 ± 41.80 | 0.83 |
| AST (IU/liter) | 64.94 ± 27.63 | 58.17 ± 23.98 | 0.44 |
| HCV-RNA (IU/ml) | 84,290 ± 186,300 | 501,800 ± 816,700 | 0.07 |

[a] Values are means ± standard deviations. SVR, sustained virological response; BMI, body mass index; WBC, white blood cell; ALT, alanine aminotransferase; AST, aspartate aminotransferase.

**Correlation between NS5A sequence heterogeneity and SVR in HCV-4 infection.** We and other researchers reported significant correlation between sequence polymorphisms within the C-terminal half of NS5A, including that in ISDR and IRRDR, and PEG-IFN/RBV treatment outcome in HCV-1 and HCV-2 infections (13, 15, 18, 30). However, this information is quite limited in HCV-4 infection. To clarify this issue, part of the HCV-4 genome encoding a carboxy terminus (aa 2193 to 2417) of NS5A in pretreatment sera was amplified and sequenced, and amino acid sequences were deduced. The sequences obtained as well as all available NS5A sequences of HCV-4a, -4m, -4n, and -4o from the databases were aligned, and the consensus sequences for a desired HCV-4 subtype were inferred (see Materials and Methods). Next, to identify an NS5A region(s) that would be significantly correlated with treatment outcome, we carried out a sliding window analysis with a window size of 30 residues over the C-terminal half (aa 2193 to 2417) of NS5A sequences obtained from all SVR ($n$ = 25) and non-SVR ($n$ = 18) patients along with corresponding consensus sequences of each HCV-4 subtype as described previously (30). This analysis revealed that the difference in the overall number of amino acid mutations between SVR and non-SVR isolates exceeded the significant threshold only in a region corresponding to IRRDR of HCV-1b (13), ranging from aa 2331 to 2383, thus being referred to as IRRDR[HCV-4] (Fig. 1). Indeed, the average number of amino acid mutations in IRRDR[HCV-4] was significantly larger in SVR than in non-SVR ($P$ = 0.0005) isolates (Fig. 2A). Sequences of IRRDR of HCV-4a, -4m, -4n, and -4o obtained from SVR and non-SVR patients along with the number of IRRDR mutations of each isolate are shown in Fig. 2B.

Next, we performed ROC curve analysis to estimate the optimal cutoff number of IRRDR[HCV-4] mutations for SVR prediction. This analysis estimated 4 mutations as the optimal number of IRRDR[HCV-4] mutations to predict SVR, since it achieved the highest sensitivity (84%; sensitivity refers to the proportion of SVR patients who were infected with HCV isolates of IRRDR[HCV-4] with 4 or more mutations) and specificity (72%; specificity refers to the proportion of non-SVR patients who were infected with HCV isolates of IRRDR[HCV-4] with 3 or fewer mutations) with an area under the curve (AUC) of 0.82 (Fig. 3). Accordingly, 21 (84%) of 25 patients with SVR, in contrast to only 5 (28%) of 18 patients with non-SVR, had IRRDR[HCV-4] with 4 or more mutations (referred to as IRRDR[HCV-4]≥4), with the difference between the two groups being statistically significant ($P$ = 0.0004) (Table 3). It should be noted that 4 (31%) of 13 patients with null response and only 1 (20%) of 5 patients with relapse had HCV with IRRDR[HCV-4]≥4. These results collectively suggest that IRRDR[HCV-4]≥4 is significantly associated with SVR. In this connection, we also tested the impact of a higher (≥5) and a lower (≥3) degree of IRRDR mutations on treatment outcome. IRRDR[HCV-4]≥5 was significantly associated with SVR, though with a relatively lower sensitivity (64%) than that of IRRDR[HCV-4]≥4 (Table 3). On the other hand, there was no significant correlation between IRRDR[HCV-4]≥3 and SVR.

**Correlation between core protein sequence heterogeneity and SVR in HCV-4 infection.** A close correlation between core protein sequence patterns at positions 70 and 91 and treatment outcome has been proposed, especially in Japanese patients with HCV-1b infection (4–6). To examine this hypothesis in Egyptian patients infected with HCV-4, core sequences of the viral genome were amplified from the pretreated sera, and the amino acid sequences were deduced. Due to a high degree of sequence homology among core sequences of various HCV-4 subtypes, all sequences obtained were aligned with the prototype sequence, ED43 (10). The residues at positions 70 and 91 were both well conserved among the sequences analyzed, and therefore, no correlation with treatment outcome was observed for these residues (Fig. 4). All but two isolates had arginine at position 70 ($Arg^{70}$), the residue that has been associated with an IFN-sensitive phenotype as far as the core protein of HCV-1b is concerned (4–6). On the other hand, Pro at position 71 showed a tendency to be more frequent in SVR than in non-SVR patients; however, the frequency was not statistically different between the two groups.

**Identification of independent predictive factors for SVR in HCV-4 infection.** In order to identify significant independent

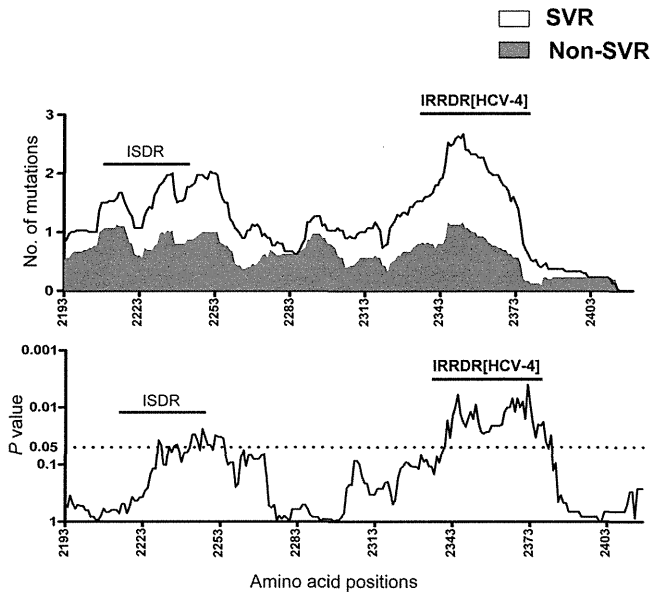


FIG 1 Sliding window analysis over the carboxy terminus (aa 2193 to 2417) of NS5A of HCV-4 obtained from SVR and non-SVR patients.

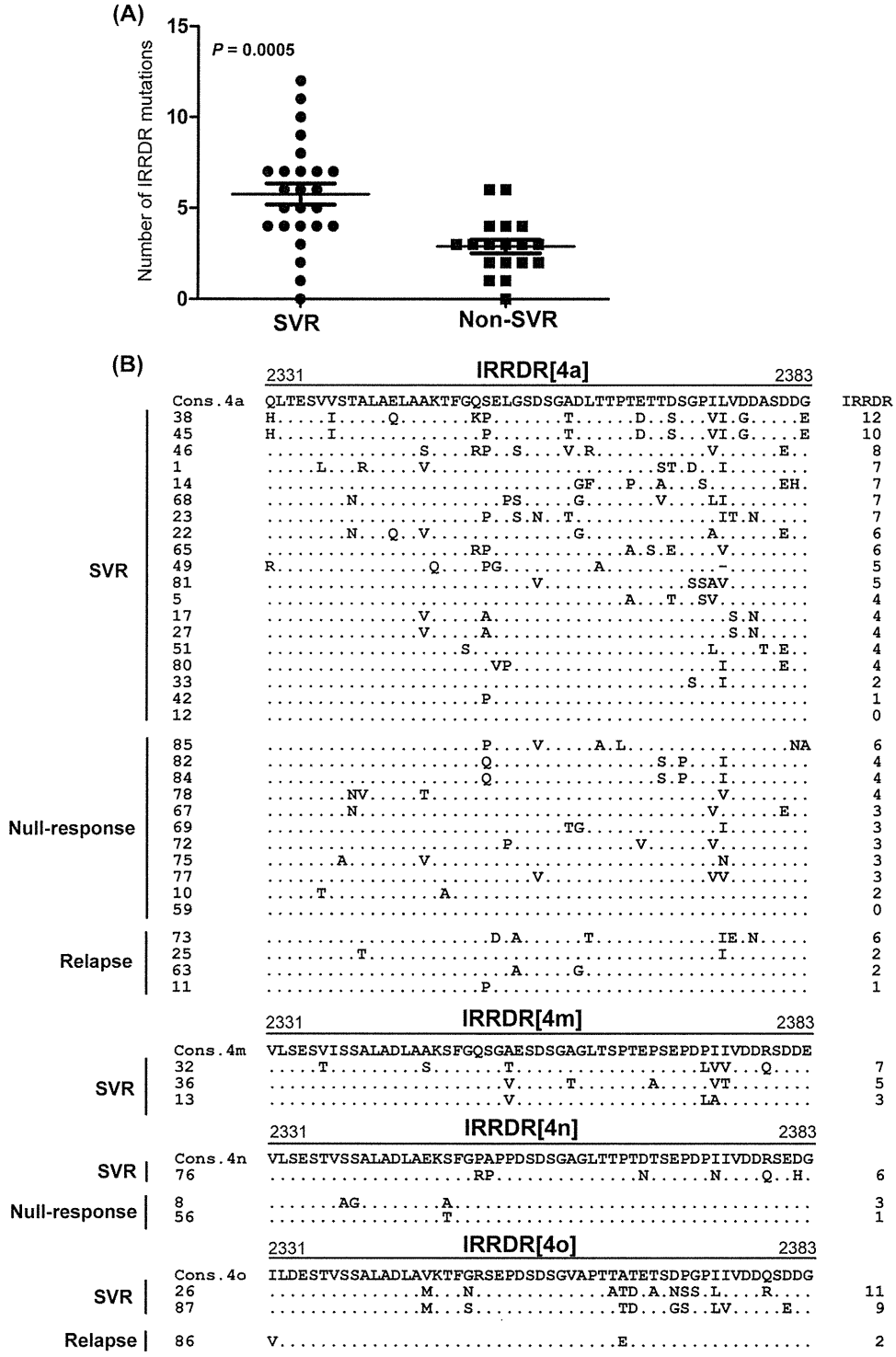


FIG 2 Correlation between IRRDR[HCV-4] sequence variations and treatment outcome. (A) Average number of amino acid mutations in IRRDR[HCV-4] obtained from SVR and non-SVR patients. (B) Alignment of IRRDR[HCV-4] sequences obtained from SVR and non-SVR patients with HCV-4a, -4m, -4n, and -4o. The consensus sequence (Cons) of each subtype is shown on the top. The numbers along the sequence indicate the amino acid positions. Dots indicate residues identical to those of the Cons sequence. The numbers of the mutations in each IRRDR (4a, 4m, 4n, or 4o) are shown on the right.

predictive factors of SVR for PEG-IFN/RBV treatment outcome in HCV-4 infection, first, all available data of baseline patients' parameters and IRRDR[HCV-4] polymorphism were entered in a univariate logistic analysis. This analysis yielded 3 factors that were correlated or nearly correlated with SVR: IRRDR[HCV-4]≥4 ($P = 0.0004$), patient's age (<42 years; $P = 0.03$), and HCV RNA titer (<5,200 IU/ml; $P = 0.08$). Subsequently, these 3 factors were entered in multivariate logistic regression analysis. This anal-

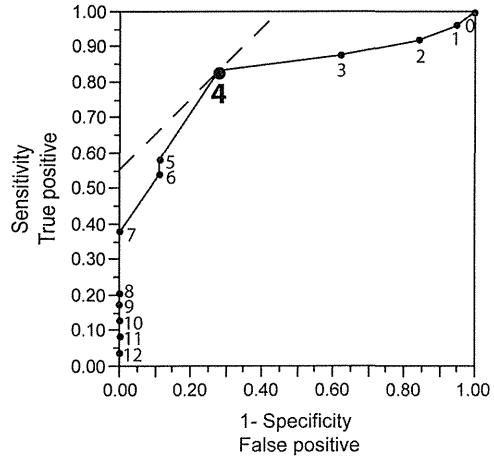


FIG 3 ROC curve analysis of IRRDR[HCV-4] sequence heterogeneity for SVR prediction. The solid line curve shows the AUC. Solid circles with numerals plotted on the curve represent different numbers of IRRDR mutations analyzed. The dashed line in the upper left corner indicates the optimal number of IRRDR[HCV-4] mutations for SVR prediction, which yields the highest sensitivity (84%) and the highest specificity (72%).

ysis revealed that the IRRDR[HCV-4]≥4 was the only independent predictive factor for SVR in HCV-4 infection (Table 4). We then assessed SVR predictability by means of IRRDR[HCV-4]≥4. As shown in Table 5, IRRDR[HCV-4]≥4 would predict SVR with a positive predictive value (PPV) of 81% ($P$ = 0.002) and sensitivity of 84%. On the other hand, IRRDR[HCV-4]≤3 would predict non-SVR with a negative predictive value (NPV) of 76% ($P$ = 0.02) and specificity of 72%. Thus, the degree of sequence variation in IRRDR[HCV-4] would yield useful positive and negative predictive markers for PEG-IFN/RBV therapy outcome in HCV-4-infected patients.

## DISCUSSION

Both host and viral genetic factors have been implicated in influencing the clinical response to PEG-IFN/RBV therapy for HCV infection (22). It has recently been reported that host genetic polymorphisms near or within the IL28B gene on chromosome 19 show a critical impact on the treatment outcome of patients infected with HCV-1 (20, 37, 39). As for the viral factor(s), polymorphisms of NS5A and core regions of a given HCV genotype have been linked to a difference in SVR rates (3, 4, 13, 18, 30). This hypothesis was mostly inferred from studies carried out with Asian populations, in particular Japanese, with HCV-1b infection. However, whether it can be applied to non-Asian populations infected with non-HCV-1 is still unknown. To the best of our knowledge, this is the first study that specifically examines the relationship between HCV genome heterogeneity, in particular in NS5A and core regions, and PEG-IFN/RBV treatment outcome in Egyptian patients infected with HCV-4. In analogy with our previous studies that identified IRRDR as a significant determinant for PEG-IFN/RBV treatment outcome in Japanese patients infected with HCV-1b, -2a, and -2b (12–16), we have demonstrated in the present study that sequence heterogeneity within IRRDR is closely associated with the ultimate treatment outcome in Egyptian patients infected with HCV-4. A high degree of sequence variation in IRRDR[HCV-4], i.e., more than 4 (IRRDR ≥ 4), significantly correlated with SVR, while a low degree of sequence variation in this region (IRRDR ≤ 3) correlated with non-SVR, null response, and relapse. The majority of patients with SVR (84%) had HCV with IRRDR of ≥4. In contrast, nearly two-thirds (72%) of the patients with non-SVR had HCV with IRRDR ≤ 3 ($P$ = 0.0004) (Table 3). Notably, 21 of the 26 patients infected with HCV with IRRDR[HCV-4]≥4 achieved SVR. Accordingly, the PPV and NPV of IRRDR[HCV-4]≥4 for SVR and non-SVR patients were 81% ($P$ = 0.002) and 76% ($P$ = 0.02), respectively (Table 5). Our present results thus strongly suggest that the degree of sequence heterogeneity within IRRDR[HCV-4] would be a useful marker for prediction of treatment outcome in HCV-4 infection.

The molecular mechanism underlying the possible involvement of this region in IFN responsiveness of the virus is still unknown. The significant difference among IRRDR sequence patterns may suggest genetic flexibility of this region. Indeed, the C-terminal portion of NS5A was shown to tolerate sequence insertions and deletions (29). This flexibility might play an important role in modulating the interaction with various host systems, including IFN-induced antiviral machineries. It is also possible that the genetic flexibility of IRRDR is accompanied by compensatory changes elsewhere in the viral genome and that these compensatory changes affect overall viral fitness and responses to IFN-based therapy (8, 29, 41). Also, it is worth noting that IRRDR is among the most variable sequences across the different genotypes and subtypes of HCV (25) whereas its upstream and downstream sequences show a higher degree of sequence conservation (15). This may suggest that whereas the upstream and downstream sequences have a conserved function(s) across all the HCV genotypes, IRRDR sequences have a genotype-dependent or even a strain-dependent function(s).

A mutation at position 70 of the core protein of HCV-1b has been reported to be correlated with PEG-IFN/RBV treatment out-

TABLE 3 Correlation between NS5A sequence heterogeneity and virological responses in HCV-4 infection

| Factor | No. of isolates/total no. (%) | | | | $P$ value for SVR versus: | | |
|---|---|---|---|---|---|---|---|
| | SVR | Non-SVR | Null response | Relapse | Non-SVR | Null response | Relapse |
| IRRDR ≥ 4 | 21/25 (84)[a] | 5/18 (28) | 4/13 (31) | 1/5 (20) | 0.0004 | 0.003 | 0.01 |
| IRRDR ≤ 3 | 4/25 (16) | 13/18 (72)[b] | 9/13 (69) | 4/5 (80) | | | |
| IRRDR ≥ 5 | 16/25 (64)[a] | 2/18 (11) | 1/13 (8) | 1/5 (20) | 0.0006 | 0.002 | 0.14 |
| IRRDR ≤ 4 | 9/25 (36) | 16/18 (89)[b] | 12/13 (92) | 4/5 (80) | | | |
| IRRDR ≥ 3 | 22/25 (88)[a] | 11/18 (61) | 10/13 (77) | 1/5 (20) | 0.066 | 0.39 | 0.006 |
| IRRDR ≤ 2 | 3/25 (12) | 7/18 (39)[b] | 3/13 (23) | 4/5 (80) | | | |

[a] Sensitivity (proportion of SVR patients with the favorable factor).
[b] Specificity (proportion of non-SVR patients with the unfavorable factor).

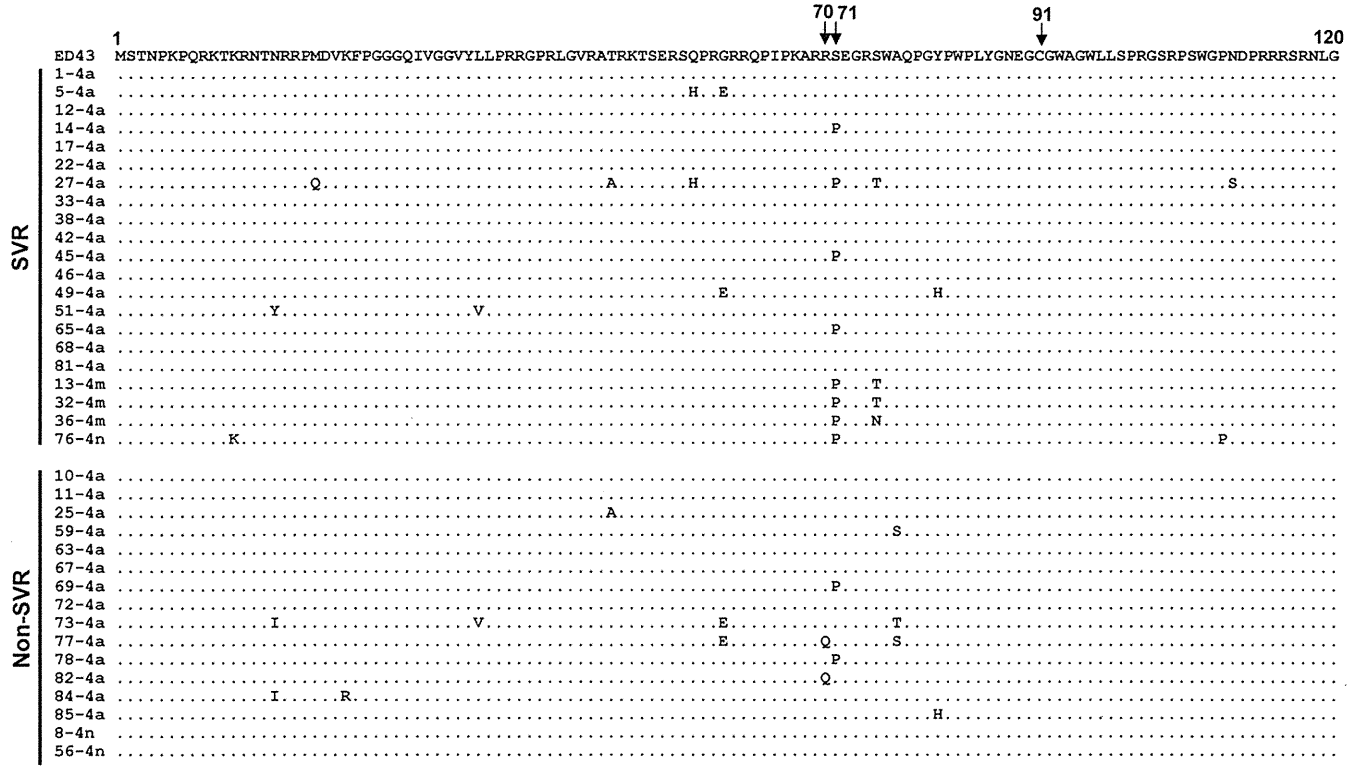


FIG 4 Sequence alignment of the core protein of HCV-4 isolates. Core protein sequences (aa 1 to 120) of HCV-4 obtained from SVR and non-SVR patients are aligned. The prototype sequence of ED43 (10) is shown on the top. The numbers along the sequence indicate the amino acid positions. Dots indicate residues identical to those of the prototype sequence.

come (4, 12). In the present study, however, we found no significant correlation between core protein polymorphism and treatment outcome in HCV-4 infection. The residue at position 70 of the core protein of all but two HCV-4 isolates analyzed in this study was Arg (Fig. 4), which is known to be associated with SVR in HCV-1b infection (4, 12). This high degree of sequence conservation at position 70 might be the reason for the lack of significant correlation between core protein polymorphism and treatment outcome in HCV-4 infection.

Single nucleotide polymorphisms (SNPs) near the IL28B region have been identified as the strongest baseline predictors of SVR to PEG-IFN/RBV in patients with HCV-1 infection. More recently, in two major studies that were carried out exclusively with HCV-4-infected patients (9, 11), the CC genotype of rs12979860 IL28B SNP was also strongly associated with SVR. It is worth noting that although the SVR rate was more than 80% among the patients with the CC genotype, these patients represented only around 40% of total SVR cases in both studies. Furthermore, the CC genotype was found in only 34% of all Egyptian patients analyzed (9). Taken together, those observations support the idea that in addition to IL28B polymorphism, there should be an additional factor(s) that influences SVR. In this context, an interplay between IRRDR and IL28B polymorphisms might explain why some patients with undesirable IL28B genotype achieve SVR and why some patients infected with HCV isolates with IRRDR[HCV-4]≥4 do not achieve SVR. Further comprehensive study is needed to validate the importance of IRRDR and IL28B polymorphisms in predicting the treatment outcome of HCV-4-infected patients.

In conclusion, the present study emphasizes the importance of IRRDR sequence heterogeneity in the prediction of PEG-IFN/RBV treatment outcome for different HCV genotype infections in

TABLE 4 Univariate and multivariate analyses for identification of independent predictive factors for SVR in HCV-4-infected patients treated with PEG-IFN/RBV therapy

| Univariate analysis | | Multivariate analysis | |
|---|---|---|---|
| Variable | *P* value | Odds ratio (95% CI) | *P* value |
| IRRDR mutations (IRRDR ≥ 4 versus IRRDR ≤ 3) | 0.0004 | 10.5 (1.12–98.91) | 0.04 |
| Age (<42 years) | 0.03 | | |
| HCV-RNA (<5,200 IU/ml) | 0.08 | | |

TABLE 5 PPV, NPV, sensitivity, and specificity of IRRDR sequence heterogeneity on the likelihood of achieving SVR and non-SVR in HCV-4 infection

| Factor | PPV | NPV | Sensitivity[c] | Specificity[d] |
|---|---|---|---|---|
| IRRDR ≥ 4 | 81% (21/26)[a] | | 84% (21/25) | |
| IRRDR ≤ 3 | | 76% (13/17)[b] | | 72% (13/18) |

[a] $P = 0.002$.
[b] $P = 0.02$.
[c] Proportion of SVR patients who were infected with HCV isolates with IRRDR of ≥4.
[d] Proportion of non-SVR patients who were infected with HCV isolates with IRRDR of ≤3.

different ethnic groups, including Egyptian patients infected with HCV-4.

## ACKNOWLEDGMENTS

This study was supported in part by Health and Labor Sciences Research Grants from the Ministry of Health, Labor and Welfare, Japan, and a SATREPS Grant from Japan Science and Technology Agency (JST) and Japan International Cooperation Agency (JICA).

This study was also carried out as part of Japan Initiative for Global Research Network on Infectious Diseases (J-GRID), Ministry of Education, Culture, Sports, Science and Technology, Japan, and the Global Center of Excellence (G-COE) Program at Kobe University Graduate School of Medicine.

No conflicts of interest exist.

## REFERENCES

1. **Abdel-Aziz F, et al.** 2000. Hepatitis C virus (HCV) infection in a community in the Nile Delta: population description and HCV prevalence. Hepatology **32**:111–115.
2. **Abdel-Hamid M, et al.** 2007. Genetic diversity in hepatitis C virus in Egypt and possible association with hepatocellular carcinoma. J. Gen. Virol. **88**:1526–1531.
3. **Akuta N, et al.** 2009. Association of amino acid substitution pattern in core protein of hepatitis C virus genotype 2a high viral load and virological response to interferon-ribavirin combination therapy. Intervirology **52**: 301–309.
4. **Akuta N, et al.** 2007. Predictive factors of early and sustained responses to peginterferon plus ribavirin combination therapy in Japanese patients infected with hepatitis C virus genotype 1b: amino acid substitutions in the core region and low-density lipoprotein cholesterol levels. J. Hepatol. **46**: 403–410.
5. **Akuta N, et al.** 2007. Prediction of response to pegylated interferon and ribavirin in hepatitis C by polymorphisms in the viral core protein and very early dynamics of viremia. Intervirology **50**:361–368.
6. **Akuta N, et al.** 2005. Association of amino acid substitution pattern in core protein of hepatitis C virus genotype 1b high viral load and non-virological response to interferon-ribavirin combination therapy. Intervirology **48**:372–380.
7. **Amoroso P, et al.** 1998. Correlation between virus genotype and chronicity rate in acute hepatitis C. J. Hepatol. **28**:939–944.
8. **Appel N, Pietschmann T, Bartenschlager R.** 2005. Mutational analysis of hepatitis C virus nonstructural protein 5A: potential role of differential phosphorylation in RNA replication and identification of a genetically flexible domain. J. Virol. **79**:3187–3194.
9. **Asselah T, et al.** 2012. IL28B polymorphism is associated with treatment response in patients with genotype 4 chronic hepatitis C. J. Hepatol. **56**: 527–532.
10. **Chamberlain RW, Adams N, Saeed AA, Simmonds P, Elliott RM.** 1997. Complete nucleotide sequence of a type 4 hepatitis C virus variant, the predominant genotype in the Middle East. J. Gen. Virol. **78**(Pt 6):1341–1347.
11. **De Nicola S, et al.** 2012. Interleukin 28B polymorphism predicts pegylated interferon plus ribavirin treatment outcome in chronic hepatitis C genotype 4. Hepatology **55**:336–342.
12. **El-Shamy A, et al.** 2012. Polymorphisms of hepatitis C virus nonstructural protein 5A and core protein and clinical outcome of pegylated-interferon/ribavirin combination therapy. Intervirology **55**:1–11.
13. **El-Shamy A, et al.** 2008. Sequence variation in hepatitis C virus nonstructural protein 5A predicts clinical outcome of pegylated interferon/ribavirin combination therapy. Hepatology **48**:38–47.
14. **El-Shamy A, et al.** 2007. Prediction of efficient virological response to pegylated interferon/ribavirin combination therapy by NS5A sequences of hepatitis C virus and anti-NS5A antibodies in pre-treatment sera. Microbiol. Immunol. **51**:471–482.
15. **El-Shamy A, et al.** 2012. Sequence heterogeneity in NS5A of hepatitis C virus genotypes 2a and 2b and clinical outcome of pegylated-interferon/ribavirin therapy. PLoS One 7:e30513. doi:10.1371/journal.pone.0030513.
16. **El-Shamy A, et al.** 2011. Sequence heterogeneity of NS5A and core proteins of hepatitis C virus and virological responses to pegylated-interferon/ribavirin combination therapy. Microbiol. Immunol. **55**:418–426.
17. **el-Zayadi AR, et al.** 2005. Hepatocellular carcinoma in Egypt: a single center study over a decade. World J. Gastroenterol. **11**:5193–5198.
18. **Enomoto N, et al.** 1996. Mutations in the nonstructural protein 5A gene and response to interferon in patients with chronic hepatitis C virus 1b infection. N. Engl. J. Med. **334**:77–81.
19. **Fried MW, et al.** 2002. Peginterferon alfa-2a plus ribavirin for chronic hepatitis C virus infection. N. Engl. J. Med. **347**:975–982.
20. **Ge D, et al.** 2009. Genetic variation in IL28B predicts hepatitis C treatment-induced viral clearance. Nature **461**:399–401.
21. **Hassan MM, et al.** 2001. The role of hepatitis C in hepatocellular carcinoma: a case control study among Egyptian patients. J. Clin. Gastroenterol. **33**:123–126.
22. **Kau A, Vermehren J, Sarrazin C.** 2008. Treatment predictors of a sustained virologic response in hepatitis B and C. J. Hepatol. **49**:634–651.
23. **Khattab MA, et al.** 2011. Management of hepatitis C virus genotype 4: recommendations of an international expert panel. J. Hepatol. **54**:1250–1262.
24. **Limaye AR, Draganov PV, Cabrera R.** 2011. Boceprevir for chronic HCV genotype 1 infection. N. Engl. J. Med. **365**:176, 177–178.
25. **Macdonald A, Harris M.** 2004. Hepatitis C virus NS5A: tales of a promiscuous protein. J. Gen. Virol. **85**:2485–2502.
26. **Maekawa S, Enomoto N.** 2009. Viral factors influencing the response to the combination therapy of peginterferon plus ribavirin in chronic hepatitis C. J. Gastroenterol. **44**:1009–1015.
27. **Mattsson L, Sonnerborg A, Weiland O.** 1993. Outcome of acute symptomatic non-A, non-B hepatitis: a 13-year follow-up study of hepatitis C virus markers. Liver **13**:274–278.
28. **Micallef JM, Kaldor JM, Dore GJ.** 2006. Spontaneous viral clearance following acute hepatitis C infection: a systematic review of longitudinal studies. J. Viral Hepat. **13**:34–41.
29. **Moradpour D, et al.** 2004. Insertion of green fluorescent protein into nonstructural protein 5A allows direct visualization of functional hepatitis C virus replication complexes. J. Virol. **78**:7400–7409.
30. **Murakami T, et al.** 1999. Mutations in nonstructural protein 5A gene and response to interferon in hepatitis C virus genotype 2 infection. Hepatology **30**:1045–1053.
31. **Okamoto H, et al.** 1992. Typing hepatitis C virus by polymerase chain reaction with type-specific primers: application to clinical surveys and tracing infectious sources. J. Gen. Virol. **73**(Pt 3):673–679.
32. **Ray SC, Arthur RR, Carella A, Bukh J, Thomas DL.** 2000. Genetic epidemiology of hepatitis C virus throughout Egypt. J. Infect. Dis. **182**: 698–707.
33. **Sarasin-Filipowicz M.** 2010. Interferon therapy of hepatitis C: molecular insights into success and failure. Swiss Med. Wkly. **140**:3–11.
34. **Sherman KE, et al.** 2011. Response-guided telaprevir combination treatment for hepatitis C virus infection. N. Engl. J. Med. **365**:1014–1024.
35. **Simmonds P, et al.** 2005. Consensus proposals for a unified system of nomenclature of hepatitis C virus genotypes. Hepatology **42**:962–973.
36. **Simmonds P, et al.** 1993. Classification of hepatitis C virus into six major genotypes and a series of subtypes by phylogenetic analysis of the NS-5 region. J. Gen. Virol. **74**(Pt 11):2391–2399.
37. **Suppiah V, et al.** 2009. IL28B is associated with response to chronic hepatitis C interferon-alpha and ribavirin therapy. Nat. Genet. **41**:1100–1104.
38. **Tanaka E, Kiyosawa K.** 2000. Natural history of acute hepatitis C. J. Gastroenterol. Hepatol. **15**(Suppl):E97–E104.
39. **Tanaka Y, et al.** 2009. Genome-wide association of IL28B with response to pegylated interferon-alpha and ribavirin therapy for chronic hepatitis C. Nat. Genet. **41**:1105–1109.
40. **Timm J, et al.** 2007. Characterization of full-length hepatitis C virus genotype 4 sequences. J. Viral Hepat. **14**:330–337.
41. **Yuan HJ, Jain M, Snow KK, Gale M, Jr, Lee WM.** 2010. Evolution of hepatitis C virus NS5A region in breakthrough patients during pegylated interferon and ribavirin therapy. J. Viral Hepat. **17**:208–216.

OPEN ACCESS Freely available online

PLOS ONE

# HCV NS5A Protein Containing Potential Ligands for Both Src Homology 2 and 3 Domains Enhances Autophosphorylation of Src Family Kinase Fyn in B Cells

**Kenji Nakashima[1], Kenji Takeuchi[1,2], Kazuyasu Chihara[1,2], Tomoko Horiguchi[1], Xuedong Sun[1], Lin Deng[3], Ikuo Shoji[3], Hak Hotta[3], Kiyonao Sada[1,2]***

**1** Division of Genome Science and Microbiology, Department of Pathological Sciences, School of Medicine, Faculty of Medical Sciences, University of Fukui, Eiheiji, Japan, **2** Organization for Life Science Advancement Programs, University of Fukui, Eiheiji, Japan, **3** Division of Microbiology, Center for Infectious Diseases, Kobe University Graduate School of Medicine, Kobe, Japan

## Abstract

Hepatitis C virus (HCV) infects B lymphocytes and induces mixed cryoglobulinemia and B cell non-Hodgkin's lymphoma. The molecular mechanism for the pathogenesis of HCV infection-mediated B cell disorders remains obscure. To identify the possible role for HCV nonstructural 5A (NS5A) protein in B cells, we generated the stable B cell lines expressing Myc-His tagged NS5A. Immunoprecipitation study in the presence or absence of pervanadate (PV) implied that NS5A was tyrosine phosphorylated by pervanadate (PV) treatment of the cells. Therefore we examined pull-down assay by using glutathione S-transferase (GST)-fusion proteins of various Src homology 2 (SH2) domains, which associates with phosphotyrosine within a specific amino acid sequence. The results showed that NS5A specifically bound to SH2 domain of Fyn from PV-treated B cells in addition to Src homology 3 (SH3) domain. Substitution of $Arg^{176}$ to Lys in the SH2 domain of Fyn abrogated this interaction. Deletion mutational analysis demonstrated that N-terminal region of NS5A was not required for the interaction with the SH2 domain of Fyn. $Tyr^{334}$ was identified as a tyrosine phosphorylation site in NS5A. Far-western analysis revealed that SH2 domain of Fyn directly bound to NS5A. Fyn and NS5A were colocalized in the lipid raft. These results suggest that NS5A directly binds to the SH2 domain of Fyn in a tyrosine phosphorylation-dependent manner. Lastly, we showed that the expression of NS5A in B cells increased phosphorylation of activation loop tyrosine in the kinase domain of Fyn. NS5A containing ligand for both SH2 and SH3 domains enhances an aberrant autophosphorylation and kinase activity of Fyn in B cells.

**Citation:** Nakashima K, Takeuchi K, Chihara K, Horiguchi T, Sun X, et al. (2012) HCV NS5A Protein Containing Potential Ligands for Both Src Homology 2 and 3 Domains Enhances Autophosphorylation of Src Family Kinase Fyn in B Cells. PLoS ONE 7(10): e46634. doi:10.1371/journal.pone.0046634

**Editor:** Philippe Gallay, Scripps Research Institute, United States of America

**Received** April 12, 2012; **Accepted** September 2, 2012; **Published** October 16, 2012



**Funding:** This study was supported in part by research funding from the University of Fukui, Takeda Science Foundation, Yakult Foundation, and the Grant-in-Aids from the Japan Society for the Promotion of Science and the Ministry of Education, Culture, Sports and Technology, Japan. The funders had no role in study design, data collection and analysis, decision to publish, or preparation of the manuscript.

**Competing Interests:** The authors have declared that no competing interests exist.

* E-mail: ksada@u-fukui.ac.jp

## Introduction

HCV is a small enveloped positive-sense RNA virus classified within the family *Flaviviridae* [1,2]. In addition to liver cells, HCV infects B cells, leading to mixed cryoglobulinemia and B cell non-Hodgkin's lymphoma [3–5]. HCV infection in B cells enhances the expression of lymphomagenesis-related genes, such as activation-induced cytidine deaminase (AID) [6,7]. However, the molecular mechanisms of HCV infection-mediated B cell disorders remain elusive.

Non-receptor type of protein-tyrosine kinase Fyn is a member of the Src family kinases, and has regulatory roles in immune receptor signaling. Recently, Fyn has been recognized as an important mediator of mitogenic signaling and regulator of cell cycle entry, growth and proliferation. As for pathological aspects, Fyn is overexpressed in various cancers, and overexpression of Fyn in cultured cells resulted in cancer-like phenotypes [8].

The Src family kinases all share a common structure and pattern of activation. The domains of these proteins include SH2, SH3, and kinase domains followed by a short C-terminal regulatory tail. The SH2 and SH3 domains are highly conserved regions and mediate protein-protein interactions: the SH2 domain binds to phosphotyrosine residue within the specific amino acid sequence, while the SH3 domain recognizes proline rich regions. HCV NS5A was shown to interact with various SH3 domains of intracellular signaling molecules, and the kinase activity of Fyn was upregulated in liver cell lines harboring HCV replicon [9]. Binding of ligands to both the SH2 and SH3 domains disrupts autoinhibitory intramolecular interactions and leads to the opened conformation. Then autophosphorylation of the activation loop tyrosine ($Tyr^{420}$ in Fyn) and dephosphorylation of the C-terminal tail ($Tyr^{531}$ in Fyn) by protein-tyrosine phosphatases lead to the activation of kinase activity [10].

Previously, we reported that Syk, another non-receptor type of protein-tyrosine kinase interacts with transiently expressed NS5A in PV treated BJAB B cells [11]. This suggested that protein-tyrosine phosphorylation is required for the association of NS5A with Syk, because PV is a nonspecific inhibitor of protein-tyrosine phosphatases and treatment of cells with PV causes increase in

protein-tyrosine phosphorylation in whole cells. Recently Pfannkuche *et al.* reported that NS5A binds to the SH2 domain of Src [12]. However, molecular mechanism of their interaction and effect of NS5A on the kinase activity of Src remain unclear.

In this study, we investigated the interaction between NS5A and the SH2 domain of Fyn in B cells.

## Materials and Methods

### Antibodies and cDNAs

Anti-NS5A and anti-glyceraldehyde-3-phosphate dehydrogenase (GAPDH) mAbs were purchased from Millipore (Bedford, MA, USA). Anti-Myc mAb and anti-Fyn antibody were obtained from Santa Cruz Biotechnology (Santa Cruz, CA, USA). Anti-phosphotyrosine (pTyr) (PY20) and human anti-IgM mAbs were from Zymed (South San Francisco, CA, USA). Anti-GST mAb was from Nacalai (Kyoto, Japan). Anti-phospho-Src family (Tyr416) antibody, which detects phosphorylated amount of $Tyr^{420}$ in Fyn, was from Cell Signaling Technology (Danvers, MA, USA). The pEF1A-NS5A(Con1)-Myc-His plasmid and its deletion or substitution mutants were described previously [11]. Deletion of NS5A 127–146 (NS5A Δ127–146) was generated by the PCR-based method using four primers, 5′-TTGGTACCATGTCCGGCTCGTGGCTAAGAG-3′, 5′-GCTCTAGAGCAGCAGACGACGTCCTCA-3′, 5′-GGTTACGCGGGTGGGGGATCCCGAATTCTTCACAGAAGTG-3′, and 5′-CACTTCTGTGAAGAATTCGGGATCCCCCACCCGCGTAACC-3′, using NS5A cDNA as a template. Substitution of $Tyr^{129}$ to Phe (Y129F) of NS5A 1–146 was generated by the site-directed mutagenesis using two primers, 5′-GGGGATTTCCACTTCGTGACGGGCA-3′ and 5′-TGCCCGTCACGAAGTGGAAATCCCC-3′, using NS5A 1–146 cDNA as a template. Substitutions of $Tyr^{182}$ to Phe (Y182F), $Tyr^{321}$ to Phe (Y321F), and $Tyr^{334}$ to Phe (Y334F) of NS5A 147–447 were generated by the site-directed mutagenesis using two specific primers designed by QuikChange Primer Design Program (www.genomics.agilent.com), using NS5A 147–447 as a template. The resulted mutations were confirmed by the DNA sequencing.

### Cell culture and transfection

B-lymphoid leukemia BJAB cells were kindly provided from Dr. Satoshi Ishido (RIKEN, Yokohama, Japan) [13] and maintained as described previously [14]. For the stable transfection of BJAB cells, 6 μg of linearized pEF1A-NS5A(Con1)-Myc-His was transfected into $5\times10^6$ cells/500 μl of cells by electroporation (240 V, 950 μF). Stably transfected cell lines were selected with 0.4 mg/ml of active G418 (Wako, Osaka, Japan) [15]. Cell lines were screened by level of protein expression by immunoblotting of detergent soluble lysates with anti-NS5A and anti-GAPDH mAbs as an internal control. Two positive cloned lines were selected for further analysis. For control cells, linearized empty vector was transfected by electroporation, and pooled clones resistant to 0.4 mg/ml of active G418 were utilized as control cells. COS cells were obtained from American Type Culture Collection (Manassas, VA, USA) and Ramos-T cells were kindly provided from Dr. Hamid Band (Nebraska Medical Center, NE, USA) [16]. Transient transfection of COS cells and Ramos-T cells were described previously [17]. Huh-7.5 cells were kindly provided from Dr. Charles M. Rice (The Rockefeller University, NY, USA) [18] and stably harboring an HCV replicon (pFK5B/2884 Gly) were described previously [11].

### Cell activation, immunoprecipitation and immunoblotting

BJAB cells ($10^8$) were washed twice with serum free medium and treated with 100 μM PV or 10 μg/ml of anti-IgM mAb for 3 min at 37°C in the same medium. Either unstimulated or stimulated cells were washed twice with ice-cold PBS and then solubilized in the lysis buffer (1% Triton X-100, 50 mM Tris, pH7.4, 150 mM NaCl, 10 mM EDTA, 100 mM NaF, 1 mM $Na_3VO_4$, 1 mM phenylmethylsulfonyl fluoride and 2 μg/ml aprotinin) on ice. In some experiments, 0.5% Nonidet P-40 was used instead of 1% Triton. Precleared cell lysates were incubated with the indicated antibodies prebound to protein A-agarose beads (Sigma, St. Louis, MO, USA). After rotation for 90 min at 4°C, the beads were washed 4 times with the lysis buffer, and the immunoprecipitated proteins were eluted by the heat treatment for 5 min at 100°C with 2×sampling buffer. Precipitated proteins or cell lysates were separated by SDS-PAGE and transferred to polyvinylidene difluoride (PVDF) membrane (Millipore). After blocking in 5% milk in TBST (25 mM Tris, pH 8.0, 150 mM NaCl, and 0.1% Tween 20), the blots were incubated with the primary antibodies and then horseradish peroxidase-conjugated goat anti-rabbit IgG, goat anti-mouse IgG antibodies (Jackson ImmunoResearch Laboratories, West Grove, PA, USA), or horseradish peroxidase-conjugated protein G (Sigma) in TBST. To enhance the signals, Immuno-enhancer Reagent A (Wako) was utilized in the reaction with anti-pTyr (pY20) mAb. Finally, proteins were visualized by the enhanced chemiluminescence (ECL) reagent (Western Lightning, PerkinElmer Life Sciences, Boston, MA) [19]. Immunoblot quantification was performed using the program Scion Image (Scion, Frederick, MD, USA).

### Pull-down assay

The cDNA for Fyn-SH2 ($Trp^{149}$-$Ala^{257}$) and –SH3 ($Thr^{82}$-$Glu^{148}$) were amplified by PCR using paired primers 5′-GGAATTCATGGTACTTTGGAAAACTTGGC-3′ and 5′-CCGCTCGAGATCTTTAGCCAATCCAGAAGT-3′ for –SH2, 5′-GGAATTCAACAGGAGTGACACTGTTTGTG-3′ and 5′-CCGCTCGAGCTCTTCTGCCTGGATGGAGTC-3′ for –SH3, using mouse Fyn(T) cDNA (a gift from Dr. Yasuhiro Minami, Kobe University, Kobe, Japan) as a template. The cDNA for c-Abl-SH2 ($Typ^{146}$-$His^{221}$) and -SH3 ($Leu^{84}$-$Val^{138}$) were amplified by PCR using paired primers 5′-CGGAATTCCTGGTATCATGGCCCTGTATCT-3′ and 5′-ATAGTTTAGCGGCCGCTAGCTGGGTAGTGGAGTGTGGT-3′ for -SH2, 5′-CGGAATTCCCTTTTTGTGGCACTCTATGAT-3′ and 5′-TAGTTTAGCGGCCGCTGACGGGGGTGATGTAGTTGCT-3′ for -SH3, using mouse c-Abl cDNA (a gift from Dr. David Baltimore, California Institute of Technology, CA, USA) as a template. The cDNA for Cbl-b N-terminal region containing SH2 domain ($Ala^2$-$Pro^{349}$) was amplified by PCR using 5′-CGGAATTCCGCAAACTCAATGAATGGCAGA-3′ and 5′-CCGCTCGAGCTAAGGTGTAGGTTCACATAATCC-3′, using human Cbl-b cDNA (a gift form Dr. Stanley Lipkowitz, National Naval Cancer Center, MD, USA) as a template. Resulted PCR fragments were subcloned into pGEX-4T.3 (GE Healthcare, Piscataway, NJ, USA) to make domain in-frame with the downstream of GST and verified by DNA sequencing. The GST-rat Lyn-SH2 and Syk-SH2 (N+C) expression constructs were provided by Dr. Reuben P. Siraganian (National Institutes of Health, MD, USA). Preparation of GST-rat Vav1-SH2, mouse c-Abl SH3 domain-binding protein-2 (3BP2)-SH2, human phospholipase C (PLC)-γ2-SH2 (N+C), and rat Lyn-SH3 domain expression constructs were described elsewhere [17,20,21]. Substitution of $Arg^{176}$ to Lys (R176K) by a point mutation of pGEX-

4T.3-Fyn-SH2 was generated by the site-directed mutagenesis using two primers 5′-TCAAAGAGAGCCAAACCACCAAAGG-3′ and 5′-TAAGAAAGGTACCTCTTGGGTTTCC-3′, using Fyn-SH2 cDNA wild type as a template. The resulted point mutation was confirmed by the DNA sequencing. All these SH2 and SH3 domains were fused downstream of GST. The GST fusion proteins were affinity-purified with glutathione Sepharose 4B beads (GE Healthcare). Extraction of GST-fusion proteins from bacteria was confirmed by the SDS-PAGE and Coomassie brilliant blue staining [22].

BJAB cells ($10^8$), Huh-7.5 cells stably harboring an HCV replicon ($3\times10^6$), COS cells ($10^6$) or Ramos B cells expressing SV40 T antigen (Ramos-T cells) ($10^7$) were washed twice with serum free medium and stimulated with 100 μM PV for 3 min at 37°C. Either unstimulated or stimulated cells were solubilized in the binding buffer (1% NP-40, 50 mM Tris, pH7.4, 150 mM NaCl, 10 mM EDTA, 100 mM NaF, 1 mM $Na_3VO_4$, 1 mM phenylmethylsulfonyl fluoride and 2 μg/ml aprotinin). After centrifugation, the resulted supernatants were reacted with 20 μg of GST-fusion proteins prebound to glutathione Sepharose 4B beads for 90 min at 4°C. The beads were washed 4 times with the binding buffer. Proteins interacting with GST-fusion proteins were eluted by heat treatment for 5 min at 100°C with 2×sampling buffer, separated by SDS-PAGE, and analyzed by immunoblotting.

### Far-western

Anti-NS5A immunoprecipitates from BJAB cells ($3\times10^7$) were separated by SDS-PAGE and transferred to PVDF membrane. After blocking, the membranes were incubated with 2.5 μg/ml of GST or GST-Fyn-SH2 for 1 h at 4°C. After extensive washing, membranes were reacted with anti-GST mAb, subsequently reacted with horseradish peroxidase conjugated goat anti-mouse IgG antibody, and then subjected to ECL detection [17].

### Subcellular fractionation

The low density detergent-insoluble fractions were prepared by sucrose density gradient centrifugation as described [23]. BJAB cells ($10^8$) were solubilized in 2.5 ml of 0.05% Triton in MNEV buffer (150 mM NaCl, 25 mM Mes, pH 6.5, 5 mM EDTA, 1 mM $Na_3VO_4$, and protease inhibitors) and dounced 10 times. Homogenates were cleared of intact cells by centrifugation for 10 minutes at 200 *g*. The resultant supernatants (2.4 ml) were mixed with equal volumes of 80% sucrose in MNEV buffer (final, 40% sucrose and 0.025% Triton), overlayered by 4.8 ml 30% and 2.4 ml 5% sucrose in MNEV buffer, and then centrifuged for 20 hours at 200 000 *g* (P40ST rotor, Himac CP80WX, Hitachi, Tokyo, Japan). After sucrose density gradient centrifugation, 9 fractions were collected from the top of the gradient and analyzed by the immunoblotting.

### Statistical analysis

Quantification of Fyn was analyzed by ImageJ software. The two-tailed Student t-test was applied to evaluate the statistical significance of differences found. A $P$ value of $<0.05$ was considered statistically significant.

### *In vitro* kinase assay

Unstimulated BJAB cells were washed twice with ice-cold PBS and then solubilized in the lysis buffer. Precleared cell lysates were incubated with anti-Fyn antibody prebound to protein A-agarose beads. After rotation for 90 min at 4°C, the beads were washed 4 times with the lysis buffer, 2 times with the kinase buffer without ATP, then incubated with 20 μl of the kinase buffer (40 mM Hepes, pH 7.5, 10 mM $MgCl_2$, 2 mM $MnCl_2$, 4 μM ATP, 4 μCi [$\gamma$-$^{32}$P] ATP) and 2.5 μg of acid-treated enolase (Sigma) for 30 min at room temperature. Reaction was terminated and proteins were eluted by the heat treatment for 5 min at 100°C with 2×sampling buffer. Proteins were separated by SDS-PAGE and gel was incubated with 1N KOH for 1 h at 56°C to remove phosphoserine and most of phosphothreonine. After fixation, the gel was dried and radiolabeled proteins were visualized by autoradiography. Immunoprecipitation of Fyn was confirmed by the immunoblotting.

## Results

### HCV NS5A associates with the SH2 domain of Fyn

To identify HCV NS5A-interacting protein in B cells, we generated the stable B cell lines in which Myc-His tagged NS5A protein is constitutively expressed. Since we confirmed that the parental cells did not express NS5A, we choose the clones in which the level of NS5A expression was highest (Fig. 1A). In the following experiments, two cloned lines (clone 3 and 7) were examined, although some figures present the results from only one representative cell line. For control, vector plasmid was transfected into the same parental cells and G418-resistant clones were pooled and utilized as control cells.

Next, we performed immunoprecipitation study using anti-Myc mAb and found tyrosine phosphorylated proteins (Fig. 1B). This suggests that NS5A was tyrosine phosphorylated by PV treatment or another protein with similar size that associates with NS5A (Fig. 1B). Another experiment by affinity tag purification using Nickel column which could react with His-tag (His-Accept kit, Nacalai) also showed some tyrosine phosphorylated proteins in NS5A protein complex (data not shown). These findings suggest the possible involvement of protein-tyrosine phosphorylation associating with NS5A. Therefore, we tried to identify the protein which associates with NS5A through SH2 domain, which recognizes specific phosphotyrosine-containing amino acid sequence.

Then we carried out pull-down assay using GST-fusion proteins of various SH2 domains (Fig. 1C). Among these, the SH2 domain of Fyn dramatically bound to NS5A from PV-treated B cells. The SH2 domains of PLC-γ2 weakly bound to NS5A. The SH2 domains of Lyn, Abl, Vav, 3BP2, Syk or Cbl-b interacted with NS5A at very low level (long exposure, data not shown). GST-Lyn-SH3 was utilized as positive control because it was reported to interact with NS5A [9]. Therefore, this data demonstrated that HCV NS5A selectively binds to the SH2 domains of Fyn and PLC-γ2 in B cells. GST-human Fyn-SH2 also interacted with NS5A (Fig. S1). Moreover, the NS5A interaction with GST-Fyn-SH2 was observed even in the context of HCV RNA replication (Fig. 1D). Thus, HCV NS5A selectively associates with the SH2 domain of Fyn.

### NS5A binds to the SH2 domain of Fyn in a tyrosine phosphorylation-dependent manner

PV treatment of cells dramatically enhances the binding of NS5A to the SH2 domain of Fyn, but not with that of Lyn or Abl (Fig. 2A). Substitution of $Arg^{176}$ to Lys in the SH2 domain of Fyn, which caused the loss of association with phosphotyrosine residue, abrogated the binding of the SH2 domain of Fyn to NS5A (Fig. 2B). $Arg^{176}$ is located in the consensus sequence within the SH2 domains to interact with phosphotyrosine residue. On the other hand, the SH3 domain of these kinases associated with NS5A to a comparable level (Fig. 2C). These results suggest that

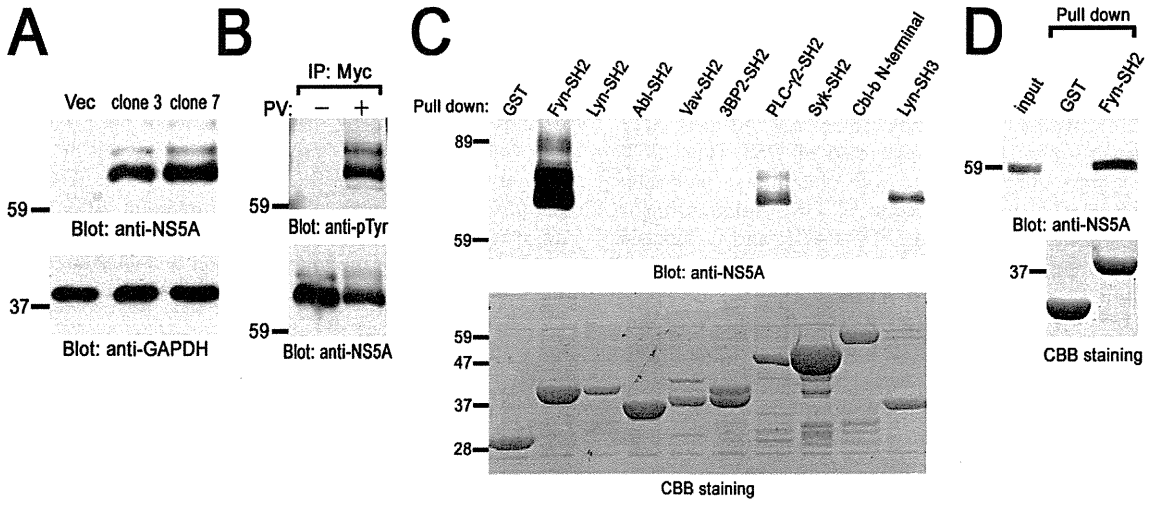


**Figure 1. Identification of HCV NS5A-interacting proteins in B cells.** (A) Generation of stable B cell lines expressing HCV NS5A. Detergent soluble cell lysates from vector cells (Vec) and Myc-His-NS5A expressing clones (clones 3 and 7) were separated by SDS-PAGE and analyzed with immunoblotting with anti-NS5A and anti-GAPDH mAbs. (B) BJAB cells expressing Myc-His-NS5A (clone 7) were treated without (−) or with (+) PV and solubilized in the lysis buffer. Cell lysates were immunoprecipitated with anti-Myc mAb and immunoprecipitated proteins were separated by SDS-PAGE and analyzed with immunoblotting with anti-pTyr (PY20) and anti-NS5A mAbs. PV-treated cells expressing Myc-His-NS5A (clone 7) (C) or Huh-7.5 cells stably harboring an HCV subgenomic replicon (D) were solubilized in the binding buffer. Precleared lysates were reacted with the indicated GST-fusion proteins and binding proteins were separated by SDS-PAGE and analyzed with immunoblotting with anti-NS5A mAb. The amount of GST-fusion proteins was confirmed by Coomassie brilliant blue (CBB) staining (C and D). Molecular sizing markers are indicated at left in kilodalton. The results were representative of three independent experiments. Similar results were obtained when another line was examined (B and C).
doi:10.1371/journal.pone.0046634.g001

increase in tyrosine phosphorylation of NS5A itself, or other associating proteins, allow the interaction with the SH2 domain of Fyn.

## Central and/or C-terminal regions of NS5A binds to the SH2 domain of Fyn

To map the Fyn-SH2-binding region in NS5A, a series of deletion mutants were examined (Fig. 3). The results obtained reveals that N-terminal region (amino acids number 1–126) is not required for the interaction with the SH2 domain of Fyn in COS cells, although this region contains the region to interact with another kinase Syk (Fig. 3A) [11]. NS5A 127–146 and 147–447 could interact with the SH2 domain of Fyn. This demonstrates that deletion of the Fyn-binding region in the context of the full-length protein leads to loss of function. Similar results were obtained when HCV NS5A proteins were transiently expressed in Ramos B cells expressing SV40 T antigen (Ramos-T cells), and examined by pull-down assay (Fig. 3B). Deletion of 127–146 (NS5A Δ127–146) still allowed binding of NS5A to the SH2

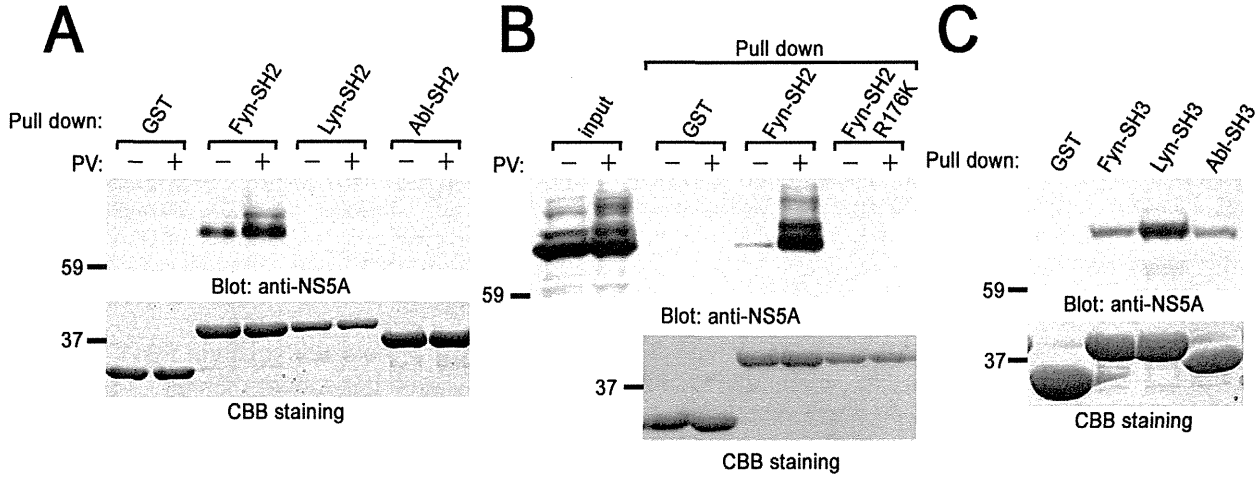


**Figure 2. Pervanadate treatment of cells stimulates the binding of NS5A to the SH2 domain of Fyn in B cells.** Either nontreated or PV-pretreated cells expressing Myc-His-NS5A (clone 7) were reacted with GST-fusion proteins of SH2 domains of various protein-tyrosine kinases (PTKs) (A), GST-Fyn-SH2 or GST-Fyn-SH2 R176K (B), or SH3 domains of various PTKs (C). Binding proteins were separated by SDS-PAGE and analyzed with immunoblotting with anti-NS5A mAb. The amount of GST-fusion proteins was confirmed by CBB staining. Molecular sizing markers are indicated at left in kilodalton. The results were representative of three independent experiments. Similar results were obtained when another line was examined.
doi:10.1371/journal.pone.0046634.g002

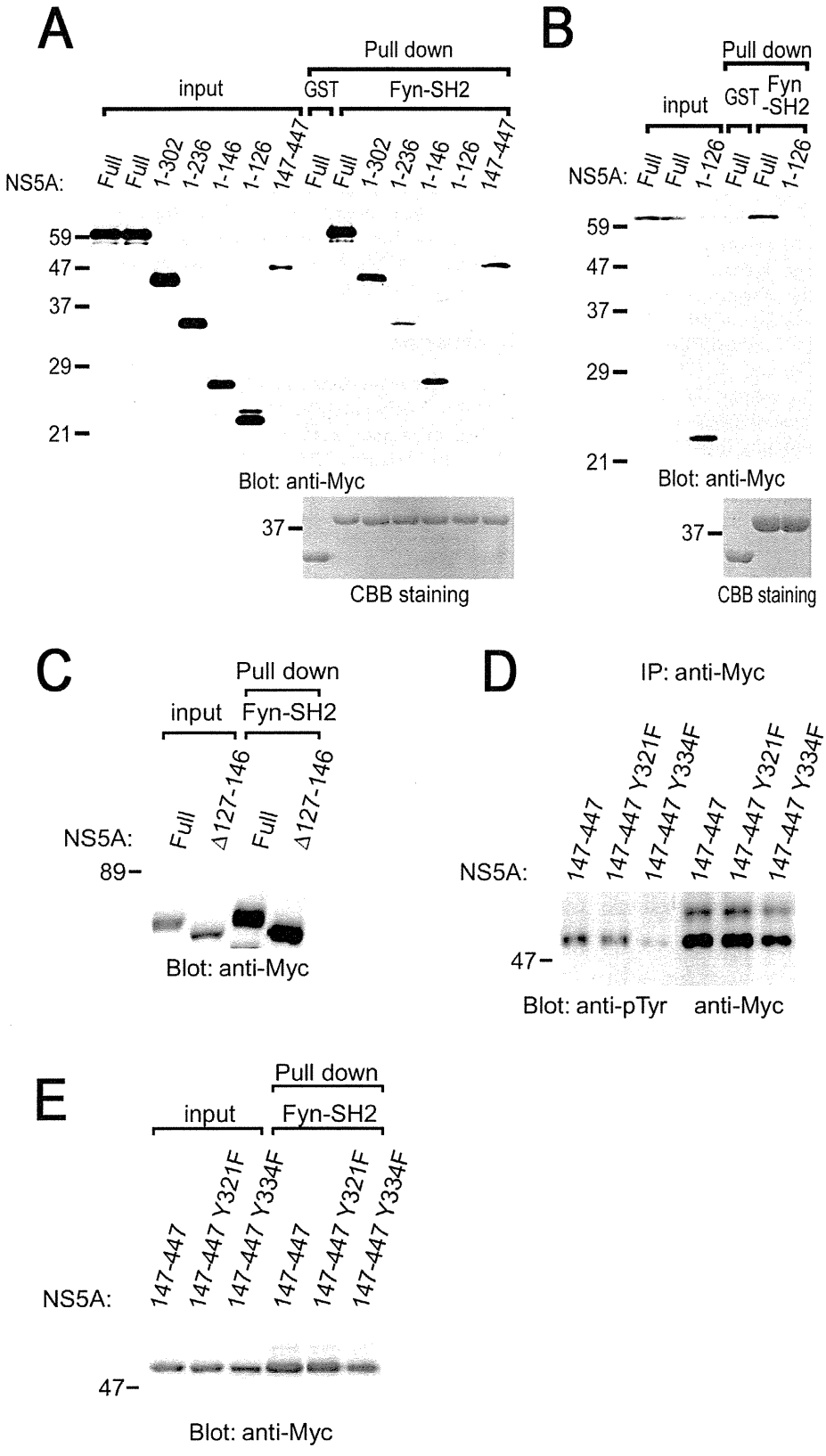


**Figure 3. Structural analysis of the association of NS5A with the SH2 domain of Fyn in B cells.** COS cells (A, C, E) or B cells (Ramos-T) (B) expressing different kinds of NS5A were stimulated with PV and subjected to pull-down assay using GST-Fyn-SH2. Binding proteins were separated by SDS-PAGE and analyzed with immunoblotting with anti-Myc mAb. The amount of GST-fusion proteins was confirmed by CBB staining. (D) COS cells expressing different kinds of NS5A mutants were stimulated with PV and subjected to immunoprecipitation. Precipitated proteins were separated by SDS-PAGE and analyzed with immunoblotting with anti-pTyr (PY20) and anti-Myc mAbs. Molecular sizing markers are indicated at left in kilodalton. The results were representative of three independent experiments.
doi:10.1371/journal.pone.0046634.g003

domain of Fyn (Fig. 3C). This suggests that NS5A Δ127–146 could interact with the SH2 domain of Fyn through NS5A 147–447.

### Identification of $Tyr^{334}$ as a tyrosine phosphorylation site in NS5A

In COS cells, full length and a series of deletion mutants of NS5A were tyrosine phosphorylated by PV treatment (Fig. S2). Because NS5A 1–126 could not bind to the SH2 domain of Fyn, we examined the possible involvement of tyrosine residue between amino acids number 127 and 146 for the binding. In this region, there is only one tyrosine residue that appears to be conserved. However, substitution of $Tyr^{129}$ to Phe of truncated NS5A (NS5A 1–146 Y129F) still allowed tyrosine phosphorylation by PV and binding to the SH2 domain of Fyn in COS cells (Fig. S2 and S3). Thus, $Tyr^{129}$ is not critical for the binding of NS5A to the SH2 domain of Fyn. In addition to this region (127 to 146), we examined the conserved tyrosine residues between 147 and 447 of NS5A ($Tyr^{182}$, $Tyr^{321}$, and $Tyr^{334}$). Among those, substitution of $Tyr^{334}$ to Phe (Y334F) reduced tyrosine phosphorylation of NS5A 147–447, however this mutant could interact with the SH2 domain of Fyn (Fig. 3D and E). NS5A Y182F and Y321F were tyrosine phosphorylated as NS5A 147–447 (Fig. 3D and data now shown). Therefore, these results suggest that $Tyr^{334}$ is required for tyrosine phosphorylation of NS5A, and existence of the multiple mechanisms for the binding of NS5A with Fyn including pTyr-SH2 domain interaction. Furthermore, we could not detect the increase in tyrosine phosphorylation of NS5A by *in vitro* kinase reaction with Fyn (data not shown), suggesting that some other protein-tyrosine kinases are required for phosphorylating NS5A.

### The SH2 domain of Fyn directly binds to NS5A

Next we examined the mechanism of the interaction of the SH2 domain of Fyn and NS5A. Association of Fyn and NS5A in B cells were tested by the immunoprecipitation study (Fig. 4A). The result showed that NS5A was coprecipitated with anti-Fyn antibody, and vice versa. Therefore, NS5A complexes with Fyn in B cells. Far-western analysis further demonstrated that the SH2 domain of Fyn could directly bind to NS5A, suggesting that NS5A is tyrosine phosphorylated in B cells (Fig. 4B). We have shown that PV treatment of cells stimulates tyrosine phosphorylation of NS5A (Fig. 1B). These results demonstrate that NS5A could be tyrosine phosphorylated in B cells and directly associated with the SH2 domain of Fyn. In addition, we demonstrated the subcellular fractionation by sucrose density gradient centrifugation (Fig. 4C). Fractions 2–4 were regarded as low density detergent-insoluble fractions, whereas 5–9 were detergent-soluble fractions. As shown, NS5A broadly located in almost all of the fractions. In contrast, most of Fyn was located in detergent-insoluble fractions because of the lipid modification of Fyn (fractions 2–4), and some were in the detergent-soluble fractions (fractions 5–9). These results demonstrate that some of NS5A and Fyn are located in low density detergent-insoluble fractions in B cells.

### Association with NS5A increases autophosphorylation and kinase activity of Fyn

Finally, we examined the effect of the expression of NS5A on the function of Fyn tyrosine kinase (Fig. 4D). Cross-linking of B cell receptor by anti-IgM mAb resulted in the increase in phosphorylation of a tyrosine residue in the activation loop of the kinase domain of Fyn, which parallels to its kinase activity [10]. Immunoprecipitation and immunoblotting experiments demonstrated that coexpression of NS5A increases phosphorylation of activation loop tyrosine and anti-IgM stimulation enhances this phenomenon. Immunoblot quantification also indicated the significant higher phosphorylation of the activation loop of Fyn in the unstimulated state in the NS5A expressing cells. In addition, we examined the biochemical kinase activity of Fyn by *in vitro* kinase assay (Fig. 4E). Coexpression of NS5A enhanced the kinase activity of Fyn as measured by both autophosphorylation and phosphorylation of exogenous substrate (enolase). This result biochemically demonstrated that association with NS5A increases tyrosine kinase activity of Fyn to phosphorylate tyrosine residues on Fyn itself and exogenous substrate. These results suggest that association of NS5A enhances an autophosphorylation and kinase activity of Fyn in B cells.

## Discussion

We have demonstrated the possible tyrosine phosphorylation of NS5A in B cells and the interaction of NS5A with the SH2 domain of Fyn, in addition to SH3 domain. Previous reports demonstrated that cells harboring HCV replicon possesses the increased kinase activity of Fyn, which supports our conclusion of this study [9]. NS5A contains a highly conserved proline rich regions with Pro-X-X-Pro-X-Arg motif which is capable of the interaction with the SH3 domains of variety of cellular proteins, including Fyn [24]. Our finding reveals the second interaction site of Fyn to associate with NS5A. Therefore, NS5A could associate with both SH3 and SH2 domains. Through the two interactions, via SH3 and SH2 domains, it is predicted that NS5A could alter the conformation of Fyn to open active state. Physiological mechanism has generally been recognized that adaptor proteins with ligands of SH2 and SH3 domains bind to Src family kinases and positively regulates the kinase activity. Consistent with previous reports, our study demonstrated that NS5A protein containing potential ligands for both SH3 and SH2 domains increases autophosphorylation of Fyn in B cells.

Fyn has two tyrosine phosphorylation sites; one tyrosine in the activation loop is phosphorylated by autophosphorylation and the other in the C-terminal tail is phosphorylated by Csk to negatively regulate the kinase activity. In this manuscript, we examine the phosphorylation of tyrosine in the activation loop by using anti-phospho-Src family (Tyr416) antibody, which detects phosphorylated amount of a conserved tyrosine in the activation loop of Src family kinase (Fig. 4D). Therefore, we could conclude that tyrosine phosphorylation of Fyn was occurred in $Tyr^{420}$ in the kinase domain.

The small interference RNA library screening study demonstrated that Csk is one of the protein-tyrosine kinases involved in the replication of HCV [25]. Csk is known to phosphorylate tyrosine residue in the C-terminal tail and negatively regulate Src family kinase, such as Fyn. Knock down of Fyn resulted in up-regulation of HCV replication [25]. This suggests that activation of Fyn suppresses HCV replication. In light of the aberrant increase in autophosphorylation of Fyn by NS5A coexpression, it is possible that NS5A negatively regulates HCV replication with activating Fyn kinase assumedly for persistent infection.

v-Src is the first discovered oncogene, and Fyn is a member of cellular Src family kinases and is also associated with cancer. Overexpression of Fyn in NIH3T3 fibroblast cells exhibited a cancer-like phonotype with increased anchorage-independent growth and prominent morphologic changes. Other studies have revealed that overexpression of Fyn results in promotion of the anti-apoptotic activity of Akt and dysregulation of anchorage-dependent cell growth. In this study, expression of NS5A enhanced autophosphorylation of Fyn in B cells, suggesting that

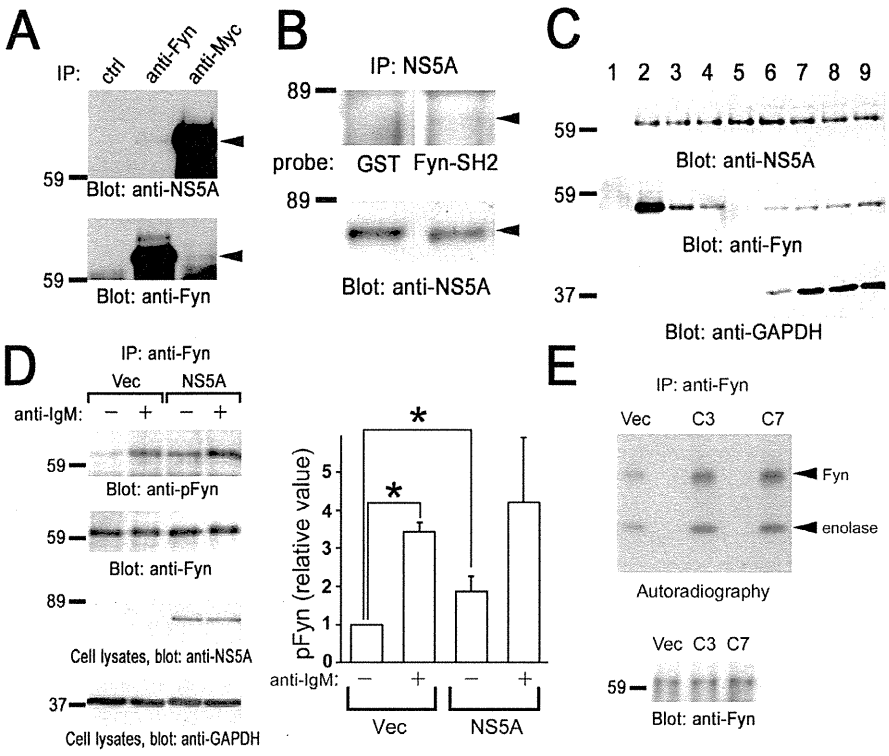


**Figure 4. Association with NS5A increases the kinase activity of Fyn in B cells.** (A) Endogenous interaction of Fyn with NS5A in BJAB cells. Cells were solubilized in the lysis buffer containing 0.5% Nonidet P-40. Detergent-soluble lysates from BJAB cells expressing Myc-His-NS5A (clone 7) were subjected to immunoprecipitation with anti-Fyn or anti-Myc antibodies. Protein interactions between NS5A and Fyn were analyzed by the immunoblotting with anti-NS5A mAb and anti-Fyn antibody, respectively. (B) Anti-Myc immunoprecipitates were separated by SDS-PAGE and subjected to far western analysis with GST or GST-Fyn-SH2 (GST-Fyn-SH2) (upper panel), and immunoblotting analysis with anti-NS5A mAb (lower panel). (C) Cell homogenates were fractionated by sucrose density gradient centrifugation. Proteins from these fractions were separated by SDS-PAGE and analyzed with immunoblotting with anti-NS5A mAb, anti-Fyn, and anti-GAPDH antibodies. (D) Control cells (Vec) and cells expressing Myc-His-NS5A (clone 7) were unstimulated (−) or stimulated (+) with anti-IgM mAb. Anti-Fyn immunoprecipitates (IP) were separated by SDS-PAGE and analyzed by immunoblotting with anti-phospho-Src family (Tyr416) antibody recognizing autophosphorylated Fyn (pFyn) and anti-Fyn antibody. Detergent-soluble lysates were separated by SDS-PAGE and analyzed by immunoblotting with anti-NS5A and anti-GAPDH mAbs. Densitometry analysis was performed on three experiments representative of Fig. 4D. Levels of pFyn were normalized to their respective total Fyn protein. The fold changes of pFyn are shown relative to unstimulated control cells. Data represent the mean ± SD of three independent experiments. *, $P<0.05$. (E) Anti-Fyn immunoprecipitates (IP) from control cells (Vec), cells expressing Myc-His-NS5A clone 3 (C3) and clone 7 (C7) were subjected to *in vitro* kinase assay using enolase as an exogenous substrate. Radioactive proteins were separated by SDS-PAGE and visualized by autoradiography. Immunoprecipitated Fyn was analyzed by immunoblotting. Molecular sizing markers are indicated at left in kilodalton. The results were representative of three independent experiments. Similar results were obtained when another line was examined.
doi:10.1371/journal.pone.0046634.g004

HCV-mediated activation of Fyn can promote aberrant growth and anti-apoptotic status leading to B lymphomagenesis [8].

Adaptor proteins have also been recognized candidates to promote oncogenes. For example, v-Crk (CT10 regulator of tyrosine kinase)/Crk-I are adaptor proteins composed of SH2 and SH3 domains but lack negative regulatory region (phosphotyrosine and C-terminal SH3 domain). Those adaptors function as constitutively activated ones, leading to tumorgenesis. Like that, NS5A presumably works constitutive activated adaptor for Fyn kinase [26].

In conclusion, present study demonstrated that NS5A binds to the SH2 domain of Fyn in tyrosine phosphorylation-dependent manner and that NS5A containing ligand for both SH2 and SH3 domains produces an aberrant increase in autophosphorylation and kinase activity of Fyn. Further studies are needed to clarify which tyrosine residues in NS5A are phosphorylated and bind to SH2 domain of Fyn. These data, however, may contribute to our understanding of the mechanisms that HCV infection causes B lymphomagenesis.

## Supporting Information

**Figure S1 GST-human Fyn-SH2 could react with NS5A.** The cDNA for human Fyn-SH2 ($Trp^{149}$-$Arg^{268}$) were amplified by PCR using paired primers 5′-GGAATTCATGGTACTTTG-GAAAACTTGGC-3′ and 5′-GATCAACTGCAGGGATTCT-CG -3′, using cDNA from total RNA of BJAB cells as a template. Resulted PCR fragment was subcloned into the pGEX-4T.3 (GE Healthcare) to make domain in-frame with the downstream of GST and verified by DNA sequencing. PV-treated cells expressing Myc-His-NS5A (clone 7) were solubilized in the lysis buffer. Precleared lysates were reacted with GST or GST-human Fyn-SH2 and binding proteins were separated by SDS-PAGE and analyzed with immunoblotting with anti-NS5A mAb. The amount of GST-fusion proteins was confirmed by CBB staining. Molecular sizing markers are indicated at left in kilodalton. The results are representative of two independent experiments.
(TIF)

**Figure S2 Tyrosine phosphorylation of NS5A and its mutants in COS cells.** Full length and a series of deletion

mutants of NS5A were transiently expressed in COS cells. Cells were unstimulated (−) or stimulated (+) with PV and solubilized in the lysis buffer. Cell lysates were immunoprecipitated with anti-Myc mAb and immunoprecipitated proteins were separated by SDS-PAGE and analyzed with immunoblotting with anti-pTyr (PY20) and anti-Myc mAbs. Molecular sizing markers are indicated at left in kilodalton. The results were representative of three independent experiments.
(TIF)

**Figure S3 $Tyr^{129}$ is not critical for the binding of NS5A to the SH2 domain of Fyn.** Indicated mutant forms of NS5A were transiently expressed in COS cells. Cells were unstimulated (−) or stimulated (+) with PV. Cells were solubilized in the binding buffer and precleared lysates were reacted with GST-Fyn-SH2. Detergent-soluble lysates and binding proteins were separated by SDS-PAGE and analyzed with immunoblotting with anti-Myc mAb. Molecular sizing markers are indicated at left in kilodalton. The results were representative of three independent experiments.
(TIF)

## Acknowledgments

We are grateful to Dr. R. Bartenschlager (University of Heidelberg, Germany) for providing an HCV subgenomic replicon (pFK5B/2884 Gly), to Ms. Satomi Nishibata and Ms. Kuniyo Miyagoshi for the assistance, and to Dr. Shinkou Kyo (Kobe University Graduate School of Medicine, Toyooka Public Hospital, Hyogo, Japan) and Dr. Keiko Kawauchi (Mechanobiology Institute, Singapore) for experimental assistance.

## Author Contributions

Conceived and designed the experiments: KN KT HH KS. Performed the experiments: KN KT TH XS KS. Analyzed the data: KN KT KC HH KS. Contributed reagents/materials/analysis tools: KN KT KC TH XS LD IS HH KS. Wrote the paper: KN HH KS.

## References

1. Moradpour D, Penin F, Rice CM (2007) Replication of hepatitis C virus. Nat Rev Microbiol 5: 453–463.
2. Suzuki T, Aizaki H, Murakami K, Shoji I, Wakita T (2007) Molecular biology of hepatitis C virus. J Gastroenterol 42: 411–423.
3. Agnello V, Chung RT, Kaplan LM (1992) A role for hepatitis C virus infection in type II cryoglobulinemia. New Engl J Med 327: 1490–1495.
4. Morsica G, Tambussi G, Sitia G, Novati R, Lazzarin A, et al. (1999) Replication of hepatitis C virus in B lymphocytes (CD19(+)). Blood 94: 1138–1139.
5. Gisbert JP, Garcia-Buey L, Pajares JM, Moreno-Otero R (2003) Prevalence of hepatitis C virus infection in B-cell non-Hodgkin's lymphoma: Systematic review and meta-analysis. Gastroenterology 125: 1723–1732.
6. Machida K, Cheng KTH, Pavio N, Sung VMH, Lai MMC (2005) Hepatitis C virus E2-CD81 interaction induces hypermutation of the immunoglobulin gene in B cells. J Virol 79: 8079–8089.
7. Ito M, Murakami K, Suzuki T, Mochida K, Suzuki M, et al. (2010) Enhanced expression of lymphomagenesis-related genes in peripheral blood B cells of chronic hepatitis C patients. Clin Immunol 135: 459–465.
8. Saito YD, Jensen AR, Salgia R, Posadas EM (2010) Fyn A Novel Molecular Target in Cancer. Cancer 116: 1629–1637.
9. Macdonald A, Crowder K, Street A, McCormick C, Harris M (2004) The hepatitis C virus NS5A protein binds to members of the Src family of tyrosine kinases and regulates kinase activity. J Gen Virol 85: 721–729.
10. Bradshaw JM (2010) The Src, Syk, and Tec family kinases: Distinct types of molecular switches. Cell Signal 22: 1175–1184.
11. Inubushi S, Nagano-Fujii M, Kitayama K, Tanaka M, An C, et al. (2008) Hepatitis C virus NS5A protein interacts with and negatively regulates the non-receptor protein tyrosine kinase Syk. J Gen Virol 89: 1231–1242.
12. Pfannkuche A, Buther K, Karthe J, Poenisch M, Bartenschlager R, et al. (2011) c-Src is required for complex formation between the hepatitis C virus-encoded proteins NS5A and NS5B: A prerequisite for replication. Hepatology 53: 1127–1136.
13. Ishido S, Choi JK, Lee BS, Wang CY, DeMaria M, et al. (2000) Inhibition of natural killer cell-mediated cytotoxicity by kaposi's sarcoma-associated herpesvirus K5 protein. Immunity 13: 365–374.
14. Ogi K, Nakashima K, Chihara K, Takeuchi K, Horiguchi T, et al. (2011) Enhancement of B-cell receptor signaling by a point mutation of adaptor protein 3BP2 identified in human inherited disease cherubism. Genes Cells 16: 951–960.
15. Sada K, Miah SM, Maeno K, Kyo S, Qu X, et al. (2002) Regulation of FcεRI-mediated degranulation by an adaptor protein 3BP2 in rat basophilic leukemia RBL-2H3 cells. Blood 100: 2138–2144.
16. Rao N, Ghosh AK, Ota S, Zhou P, Reddi AL, et al. (2001) The non-receptor tyrosine kinase Syk is a target of Cbl-mediated ubiquitylation upon B-cell receptor stimulation. EMBO J 20: 7085–7095.
17. Shukla U, Hatani T, Nakashima K, Ogi K, Sada K (2009) Tyrosine Phosphorylation of 3BP2 Regulates B Cell Receptor-mediated Activation of NFAT. J Biol Chem 284: 33719–33728.
18. Blight KJ, McKeating JA, Rice CM (2002) Highly permissive cell lines for subgenomic and genomic hepatitis C virus RNA replication. J Virol 76: 13001–13014.
19. Nakashima K, Takeuchi K, Chihara K, Hotta H, Sada K (2011) Inhibition of hepatitis C virus replication through adenosine monophosphate-activated protein kinase-dependent and -independent pathways. Microbiol Immunol 55: 774–782.
20. Maeno K, Sada K, Kyo S, Miah SM, Kawauchi-Kamata K, et al. (2003) Adaptor protein 3BP2 is a potential ligand of Src homology 2 and 3 domains of Lyn protein-tyrosine kinase. J Biol Chem 278: 24912–24920.
21. Miah SM, Hatani T, Qu X, Yamamura H, Sada K (2004) Point mutations of 3BP2 identified in human inherited disease cherubism results in the loss of function. Genes Cells 9: 993–1004.
22. Chihara K, Nakashima K, Takeuchi K, Sada K (2011) Association of 3BP2 with SHP-1 regulates SHP-1-mediated production of TNF-α in RBL-2H3 cells. Genes Cells 16: 1133–1145.
23. Qu X, Sada K, Kyo S, Maeno K, Miah SM, et al. (2004) Negative regulation of FcεRI-mediated mast cell activation by a ubiquitin-protein ligase Cbl-b. Blood 103: 1779–1786.
24. Shelton H, Harris M (2008) Hepatitis C virus NS5A protein binds the SH3 domain of the Fyn tyrosine kinase with high affinity: mutagenic analysis of residues within the SH3 domain that contribute to the interaction. Virol J 5: 24. Available: http://www.virologyj.com/content/5/1/24.
25. Supekova L, Supek F, Lee J, Chen S, Gray N, et al. (2008) Identification of human kinases involved in hepatitis C virus replication by small interference RNA library screening. J Biol Chem 283: 29–36.
26. Birge RB, Kalodimos C, Inagaki F, Tanaka S (2009) Crk and CrkL adaptor proteins: networks for physiological and pathological signaling. Cell Commun Signal 7: 13. Available: http://www.biosignaling.com/content/7/1/13.

# Mutations in non-structural 5A and rapid viral response to pegylated interferon-α-2b plus ribavirin therapy are associated with therapeutic efficacy in patients with genotype 1b chronic hepatitis C

YOSHIHIKO YANO[1,2], YASUSHI SEO[1], AKIRA MIKI[1], MASAYA SAITO[1], HIROTAKA KATO[4], KEN-ICHI HAMANO[5], MANABU OYA[6], SACHIKO OUCHI[7,8], TAKASHI FUJISAWA[8], HAJIME YAMADA[9], YUKIMASA YAMASHITA[10], SATOSHI TANI[11], SHIGEYA HIROHATA[12], SEITETSU YOON[12], NAOTO KITAJIMA[13], KAZUNARI KITAGAKI[14], AKIRA KAWARA[15], TAKATOSHI NAKASHIMA[16], HOSAI YU[17], TETSUO MAEDA[18], TAKESHI AZUMA[1], AHMED EL-SHAMY[3], HAK HOTTA[3] and YOSHITAKE HAYASHI[2]; Kobe Hepatitis Therapeutic Group

[1]Department of Gastroenterology, [2]Center for Infectious Diseases, and [3]Department of Microbiology, Kobe University Graduate School of Medicine; [4]Kato Clinic; [5]Hamano Clinic; [6]Division of Internal Medicine, Shin-Suma Hospital; [7]Division of Internal Medicine, Steel Memorial Hirohata Hospital; [8]Division of Internal Medicine, Kakogawa West City Hospital; [9]Department of Gastroenterology, Shinko Hospital; [10]Department of Gastroenterology, Kobe City Hospital Organization, Kobe City Medical Center West Hospital; [11]Division of Internal Medicine, Konan Hospital; [12]Department of Gastroenterology, Hyogo Prefectural Kakogawa Medical Center; [13]Division of Internal Medicine, Kasai City Hospital; [14]Division of Internal Medicine, Rokko-Island Hospital; [15]Kawara Clinic; [16]Department of Gastroenterology, Akashi Medical Center; [17]Division of Internal Medicine, National Hospital Organization, Kobe Medical Center; [18]Division of Internal Medicine, Kawasaki Hospital, Kobe, Japan

Received March 30, 2012; Accepted July 6, 2012

DOI: 10.3892/ijmm.2012.1093

**Abstract.** For patients chronically infected with hepatitis C virus (HCV), mutations in the non-structural 5A (NS5A) gene are important predictive factors for the response to interferon (IFN) therapy. In the present study, factor analysis of the therapeutic response of patients following pegylated IFN and ribavirin combination therapy was assessed in a multicenter study. Chronic HCV-infected patients with genotype 1b and high viral load (n=96, mean age 56.5 years; 59 males, 68 females) treated with pegylated IFN-α-2b and ribavirin combination therapy were enrolled. This study was conducted at Kobe University Hospital and 25 affiliated hospitals in Hyogo prefecture. Sixty-five patients (68%) completed treatment with both pegylated IFN and ribavirin at >80% of the weight-based scheduled dosages. Patients who reduced or terminated therapy were frequently aged women (mean age 60.8 years; 11 males, 17 females). Overall, a sustained viral response (SVR) was achieved in 42 (44%) patients out of 96. Based on per-protocol-based (PPB) analysis, the SVR rate in patients with ≥6 amino acid (aa) mutations in the IFN resistance-determining region (IRRDR) (75%) or ≥1 aa mutation in the IFN sensitivity-determining region (ISDR) (61%) was significantly higher than that in patients with <5 aa mutations in IRRDR (30%) or no mutation in ISDR (29%). Multivariate analysis revealed that rapid viral response (RVR) (odds ratio, 18.1) and mutations of ≥6 in IRRDR (odds ratio, 15.5) were significantly associated with SVR. In conclusion, mutations in the NS5A region, particularly in patients with ≥6 aa mutations in IRRDR were strongly associated with a therapeutic response to pegylated IFN and ribavirin combination therapy.

## Introduction

Hepatitis C virus (HCV) is a major cause of chronic liver disease, with an estimated 170 million people infected worldwide. In Japan, the carrier rate is estimated to be approximately 1% of the general population. This rate increases depending on age and reaches approximately 5% in individuals over 70 years of age. The main goal of treatment for chronic hepatitis C is prevention of cirrhosis and hepatocellular carcinoma by eradication of the virus. Interferon (IFN)-based therapy was initiated in 1992, and efficacy of treatment regimens has

*Correspondence to:* Dr Yoshihiko Yano, Center for Infectious Diseases, Kobe University Graduate School of Medicine, 7-5-1 Kusunoki-cho, Chuo-ku, Kobe 650-0017, Japan
E-mail: yanoyo@med.kobe-u.ac.jp

*Key words:* chronic hepatitis C, pegylated IFN and ribavirin therapy, non-structural 5A